STUDIES ON ABSORPTIVE TRANSITIONS BETWEEN ROTATIONAL SUBLEVELS OF SYMMETRIC-TOP MOLECULES IN A STATIC ELECTRIC FIELD

Thesis by

Paul George Thiene, Jr.

In Partial Fulfillment of the Requirements

for the Degree of

Doctor of Philosophy

California Institute of Technology

Pasadena, California

1952

ACKNOWLEDGMENTS

It is a pleasure to express my heartfelt gratitude to Professor W. H. Pickering, my research supervisor, for his friendly, patient guidance and continued support, not only during the course of this research, but through all the years of my graduate studies. To Professor D. M. Yost of the Chemistry Department for his interest, ready help, and kindly inspiration, I am also deeply indebted.

Several encouraging and informative discussions on questions of theory with the eminent authority Professor D. M. Dennison of the University of Michigan are gratefully acknowledged.

ABSTRACT

The topic of this research is the hitherto uninvestigated absorption of electromagnetic energy by polar symmetric-top molecules in a static electric field, which arises by virtue of direct transitions between sublevels of a single rotational state. A short theoretical treatment of the Stark effect of a rigid molecule is included. The factors governing the absorption of quanta from the surrounding radiation field are discussed in a rudimentary derivation of a formula for the maximum linear absorption coefficient of a gas.

A new microwave Stark-effect spectrometer constructed for an exploratory investigation is described. The instrument operates in an unusual manner whereby the spectral position of the absorption line is varied, while the frequency of the incident radiation is held fixed. Included also is a treatment of the factors which determine and limit the sensitivity of the spectrometer.

Experiments which strongly indicate the existence of these field-created absorption lines are reported.

CONTENTS

CONTENTS, Continued

FIGURES AND TABLES

FIGURES AND TABLES, Continued

I. INTRODUCTION

Few fields of experimental research have profited more by war-time technological advances than has spectroscopy by the World War II development of microwave techniques. "Microwave spectroscopy," virtually unknown before 1945*, is a rapidly expanding and very promising new avenue for investigating not only molecular structure, but electronic and nuclear structure as well. The possible applications are many and surprisingly varied:[2]

1. Determination of interatomic distances and molecular configurations.
2. Determination of electronic structure of molecules.
3. Study of internal rotation in molecules.
4. Calculation of thermodynamic quantities.
5. Determination of nuclear moments, spin, and statistics.
6. Determination of mass differences of isotopes.
7. Chemical and isotope analysis.
8. Studies of solids and liquids.

The region of microwave absorption spectroscopy in relation to the rest of the electromagnetic spectrum is illustrated in Figure 1. Most commonly microwaves of known frequency are passed through a test sample of the material under investigation and the absorption of energy from the incident radiation is measured. By varying the frequency of the generator and recording the corresponding power attenuation of the transmitted microwave, one determines the shape and intensity of the molecular absorption lines.

---

* Noteworthy exception is pioneer work by Cleeton and Williams in 1934 on the inversion spectrum of ammonia, reference 1.

Microwave spectroscopy affords two principal advantages over optical spectroscopy: (1) The availability of essentially monochromatic radiation sources eliminates the need of a monochromator, or dispersive element; (2) Much higher resolution* is readily obtainable, which permits study of hyperfine structure due to nuclear spins and quadrupole moments. The relationship between microwave and optical spectroscopy is not competitive, however, since the two regions of access do not overlap, as is apparent in Figure 1.

In this paper we shall be primarily concerned with the pure rotational absorption spectra of gas molecules. The mechanism by which a rotating molecule absorbs energy from a microwave is interaction between its permanent electric or magnetic dipole and the electric or magnetic field of the wave sweeping over it. So, only molecules possessing either a permanent electric or magnetic dipole moment will display pure rotational spectra. Since the electric dipole character of molecules arises from the centers of positive and negative electricity[4] of their structure being out of coincidence, a molecule such as O = C = O, for example, can have no permanent dipole moment by virtue of its symmetry.

The pure rotational energy of a rigid molecule in a stationary state depends in field-free space, not on its dipolar moment, but on its moments of inertia and on rotational quantum numbers. According to one of Bohr's postulates, the frequency or emission of absorption of a spectral line is given by

$$\nu_{ij} = \frac{1}{h}(W_j - W_i) \qquad (1)$$

---

* Approximately 10^5 times the resolution of the best infrared grating spectrometer.

W_i and W_j are the energies of the initial and final states, and h is Planck's quantum of action. Computation of the frequency of the radiation associated with a particular transition requires, then, a knowledge of the energy difference between the stationary states involved in the transition. This difference of energy may, under circumstances which are of particular concern here, be independent of the moments of inertia and depend only on the electric dipole moment of the molecule.

II. RIGID SYMMETRIC-TOP MOLECULES

A molecule composed of three or more atoms will, in general, have non-collinear nuclei. It must be treated as a rigid or semi-rigid structure having three principal moments of inertia, I_A, I_B, I_C say. So-called asymmetric-top molecules for which I_A, I_B and I_C are all different constitute the most general category. The most important degenerate class, however, is made up of molecules having an axis of symmetry, for which $I_A \neq I_B = I_C$.[5]

A. Energy of Stationary States.

While the wave-mechanical treatment of the symmetric-top molecule is not particularly difficult, it is instructive in its intuitive simplicity to consider the problem from the point of view of the classical quantum mechanics. Consider, as suggested in Figure 2, $\underset{\sim}{H}_A$ to be the angular momentum of the symmetric-top molecule about its axis of symmetry and $\underset{\sim}{H}_T$ to be the total angular momentum vector. Pure spin around the symmetry axis is not the only rotational energy possible for the top; $\underset{\sim}{H}_A$ and $\underset{\sim}{H}_T$ will not generally be coincident.

The total angular momentum vector must remain fixed, if the molecule is assumed to be in field-free space and subject to no external forces of any kind. Free precession of the top around the direction of $\underset{\sim}{H}_T$ is, however, possible; which means that in addition to the spin momentum $\underset{\sim}{H}_A$ around the axis of symmetry, there is angular momentum $\underset{\sim}{H}_T - \underset{\sim}{H}_A$ about a a principal axis normal to the symmetry axis. The total energy of the

rigid top is simply

$$W = \frac{1}{2}\frac{H_A^2}{I_A} + \frac{1}{2}\frac{H_T^2 - H_A^2}{I_B} , \tag{2}$$

which after rearrangement becomes

$$W = \frac{1}{2}\frac{H_T^2}{I_B} + \frac{1}{2}\left(\frac{1}{I_A} - \frac{1}{I_B}\right)H_A^2 . \tag{3}$$

Next, the momenta must be quantized:

$$\oint H_T\, dq_T = Jh , \quad \oint H_A\, dq_A = Kh . \tag{4}$$

q_T and q_A are the space coordinates canonically conjugate to the respective momenta, h is Planck's constant, and J and K are integers. Since the momenta are constant, the integrals give at once

$$H_T = J\hbar \qquad \text{and} \qquad H_A = K\hbar , \tag{5}$$

where $\hbar \equiv h/2\pi$. Substitution of these values in (3) yields

$$W_{JK} = \hbar B J^2 + \hbar(A - B)K^2 . \tag{6}$$

For convenience two inertial parameters (in sec^{-1}) are introduced, as is usual; namely,

$$A \equiv \frac{\hbar}{4\pi I_A} \qquad \text{and} \qquad B \equiv \frac{\hbar}{4\pi I_B} , \tag{7}$$

the "unique" and "non-unique reciprocal moments of inertia," respectively.

Equation (6) is found to agree with experiment for high values of J. For low values, a slight modification is necessary:

$$W_{JK} = hBJ(J+1) + h(A-B)K^2 \quad . \tag{8}$$

Wave mechanics[6,7] leads us directly to equation (8), as well as to the selection rules

$$\Delta J = \Delta K = 0, \pm 1 \quad .$$

In particular, for rotational absorption it is required that

$$\Delta J = +1 \, , \; \Delta K = 0 \quad .$$

Substitution of equation (6) in equation (1) in view of these conditions yields an expression for the frequency of the rotational absorption lines of a rigid symmetric-top molecule in field-free space; that is,

$$\nu_{JK}^{J+1\,K} = 2B(J+1) \quad . \tag{9}$$

While the general characteristics of microwave spectra are explicable on the basis of a rigid model, the effects of centrifugal distortion and of vibration should be considered.[8] Fortunately, if J is not too large, centrifugal distortion is negligible for symmetric-top molecules. A fraction of the molecules is, however, at room temperature in excited vibrational states, for which the moments of inertia are not quite the same as in the ground state. We should write

$$B_v = \frac{\hbar}{4\pi} \left(\frac{1}{I_B} \right)_{average} \tag{10}$$

for the average non-unique reciprocal moment of inertia for the vibrational state characterized by the quantum number v.

For reasons soon to be made apparent, the hyperfine structure which results from the quadrupole moment of the nucleus need not be considered here.[9,10]

B. Stark Effect of Rotational Levels

In the foregoing discussion it was assumed that the molecule was in field-free space. Of more interest, however, is the behavior of a polar symmetric-top molecule in a static electric field. It is helpful to refer again to a classical model; the orientation of the momenta with respect to the static electric field is shown in Figure 3. H_E is the projection of the total angular momentum vector $\underset{\sim}{H}_T$ in the direction of $\underset{\sim}{E}$, the static field intensity.

As E is increased from zero to some finite value, the molecule will, by virtue of its polar character, take up energy from the field source. If now the static field is not too strong, it is reasonable to consider as a first approximation that $\underset{\sim}{H}_T$, remaining constant in magnitude, precesses slowly about $\underset{\sim}{E}$. The time-average energy of precession is given by

$$\Delta W = -\overline{\underset{\sim}{\mu} \cdot \underset{\sim}{E}} = -\mu E \overline{\cos\theta} \quad . \tag{11}$$

The dipole moment μ of the molecule is assumed to be along the axis of symmetry. Now

$$\cos\theta = \alpha_1'\alpha_2' + \beta_1'\beta_2' + \gamma_1'\gamma_2' , \tag{12}$$

where $\alpha_1', \beta_1', \gamma_1'$, and $\alpha_2', \beta_2', \gamma_2'$ are the direction cosines of $\underset{\sim}{\mu}$ and $\underset{\sim}{E}$

with respect to the primed coordinate axes. It is apparent that as $\underset{\sim}{\mu}$, or $\underset{\sim}{H}_A$, precesses freely around $\underset{\sim}{H}_T$ and as $\underset{\sim}{H}_T$ precesses around $\underset{\sim}{E}$, γ_1' and γ_2' are time independent; while α_1' and β_1' will be periodic with a frequency which is, in general, incommensurate with that of the periodicity of α_2' and β_2'. Thus,

$$\overline{\cos\theta} = \gamma_1\gamma_2' = \frac{H_A}{H_T}\frac{H_E}{H_T} = \frac{K}{J}\frac{M}{J}, \tag{13}$$

since $\overline{\alpha_1'\alpha_2'} = \overline{\beta_1'\beta_2'} = 0$. We introduce an outer quantum number M such that $M\hbar$ is the component of the total angular momentum in the direction of the static field, which implies $-J \leq M \leq +J$. Substituting the result of equation (13) into (11) gives simply

$$\Delta W^{(1)}_{JKM} = -\mu E \frac{KM}{J^2}. \tag{14}$$ *

Wave-mechanical perturbation theory[11,12] modifies the result slightly to

$$\Delta W^{(1)}_{JKM} = -\mu E \frac{KM}{J(J+1)}. \tag{15}$$

A second-order term has been calculated by R. de Kronig[12] and others:

$$\Delta W^{(2)}_{JKM} = \frac{\mu^2 E^2}{2hB}\left\{\frac{J^2M^2(J^2-K^2)}{J^3(2J+1)(2J-1)} - \frac{[(J+1)^2-M^2][(J+1)^2-K^2]}{(J+1)^3(2J+1)(2J+3)}\right\}. \tag{16}$$

---

* A superscript (1) is attached to indicate linear dependence on E.

The second-order shift in energy levels arises from distortion of the orbital motion of the molecule by the electric field, while the first-order shift is due to forced precession of the entire molecule about the static field as we find above. It is apparent by comparing equations (15) and (16) that the first-order effect will predominate if $\mu E << 2hB$, which implies that the first-order energy perturbation is small with respect to the energy between unperturbed levels.

The first-order splitting of the levels and the allowable absorptive transitions for a symmetric-top molecule in a static electric field are shown in energy level diagrams, Figures 4 and 5. The lowest levels for a molecule in the absence of a field are plotted for comparison. Each level is resolved into $2J + 1$ sublevels by the action of the electric field. The selection rule $\Delta J = +1$ may now be expanded to include $\Delta J = 0$ transitions. It is to be noted that two distinct cases are illustrated:

1. Microwave Electric Vector Parallel to the Static Field, Figure 4.

   Only transitions $\Delta M = 0$ are allowed for this case. The absorption lines associated with these π-type transitions have been observed by means of a long wave-guide absorption cell, mounted in which is an insulated plane strip electrode parallel to the larger dimension of the guide.

   The wave guide is filled with gas and is excited in the dominant mode (TE_{01}). The molecules are subject to parallel static and microwave electric fields as shown in Figure 6. π-type transitions involve energy that clearly is of the same order as that between the

same degenerate rotational levels in the absence of the static field. By substituting equations (9) and (15) in equation (1), one finds the frequencies of the absorbed radiation to be given by

$$\nu_{KM}^{J+1\,KM} = 2B(J+1) + \frac{2\mu E}{h}\frac{KM}{J(J+1)(J+2)} \quad . \tag{17}$$

These absorption lines depend on both the non-unique reciprocal moment of inertia B and the dipole moment μ .

2. Microwave Electric Vector Perpendicular to Static Field, Figure 5.

The selection rule for the electric quantum number M is here $\Delta M = \pm 1$. Again it is apparent that transitions $\Delta J = +1$, $\Delta M = \pm 1$ involve energies comparable to the energy between the unsplit levels.

With the application of the static electric field, another set of transitions corresponding to $\Delta J = 0$ becomes possible as mentioned above. Case (1), however, requires $\Delta M = 0$, which disallows direct transitions between sublevels having the same J. In the present case this restriction is removed; consequently, direct absorptive transitions $\Delta M = -1$ between sublevels of a single rotational state are now possible. The accented arrows in Figure 5 indicate these lines.

These very interesting, hitherto uninvestigated transitions* are the particular concern of this paper. Quite unique by comparison with the

---

* Cf. Hughes, ref. 13: Investigation of second-order splitting of a diatomic linear rotator in orthogonal fields (at radio frequencies) by a molecular-beam technique.

usual $\Delta M = 0$ lines, which are merely satellites split from the unperturbed line, the $\Delta M = -1$, $\Delta J = 0$ lines are independently created from a single rotational level by the presence of the static electric field. The energy between the associated sublevels is, furthermore, small with respect to the energy of the field-free transitions. Substituting the first-order perturbation energy from equation (15) into expression (1), one obtains, in view of the selection rules,

$$\nu_{JKM}^{JKM-1} = \frac{\mu E}{h} \frac{K}{J(J+1)} \tag{18}$$

for the $\Delta M = -1$ absorption frequencies.

The exclusive appearance in the frequency expression of the molecular dipole moment, in contrast to the $\Delta M = 0$ case, is most significant. Here it seems is a means for accurately determining the dipole moment of molecules in excited states without knowledge of inertial parameters.

III. INTENSITY AND SHAPE OF ABSORPTION LINES

Since microwave radiation is exponentially absorbed in passing through a test gas, a convenient measure of the intensity of energy absorption is the linear absorption coefficient, i.e., the fractional decrease in energy per unit distance the microwave traverses the gas. In this paper, contrary to the usual convention, the shape of an absorption line is taken to mean the functional dependence of the absorption coefficient on the resonant frequency ω_i^j of a line, not on the frequency of the incident radiation.

A. Maximum Linear Absorption Coefficient

An approximate expression for the absorption coefficient of a single absorption line arising from transitions between two non-degenerate levels is readily obtainable. We start with the transition probability per unit time given by*

$$W_i^j = \frac{2}{\hbar^2 \Delta\omega} \int |H_i^j|^2 \beta \, d\omega \, . \qquad (19)$$

β is the density function of the incident microwave beam, defined so that $\beta \, d\omega$ is the number of radiation oscillators (or modes) per unit volume in the angular frequency interval ω to $\omega + d\omega$. $\Delta\omega$ is 2π times the half-width of the absorption line at half-maximum intensity. The Hamiltonian H_i^j accounts for the interaction of the radiation field

---

* W. Heitler, reference 14, page 144, equation (21) for resonance.

and the molecule; for the present case, it is simply*

$$H_{ij}' = \sqrt{2\pi\hbar\omega n}\int \psi_i^* \mu_x \psi_j \, d\tau \qquad (20)$$

for a transition between eigenstates i and j. The microwave beam is considered to have its electric vector in the X-direction and to consist of a continuum of radiation oscillators such that the occupation number n is the average number of quanta assigned to an oscillator of angular frequency ω .

In accord with the foregoing definition of the radiation density function the intensity (ergs per cm^2 sec.) of the microwave beam is

$$I(\omega)d\omega = \rho(\omega)\, d\omega\, n\hbar\omega c \qquad (21)$$

in the interval ω to $\omega + d\omega$.

Substituting $\rho(\omega)d\omega$ from (21) and H_{ij}' from (20) into (19), we obtain as the transition probability per unit time for absorption

$$w_{ij}' = \frac{4\pi}{c\hbar^2\Delta\omega}|\mu_{ij}|^2 \int I(\omega)d\omega \,, \qquad (22)$$

where μ_{ij} is the matrix element of the dipole moment operator μ_x . The integral gives, of course, the total intensity of the incident microwave beam.

In a gas at temperature T the probabilities of finding a molecule in the initial and final eigenstates are $(g_i/Z)\exp(-W_i/kT)$ and $(g_j/Z)\exp(-W_j/kT)$

---

* W. Heitler, reference 14, page 94.

where $Z \equiv \sum_i g \exp(-W_i/kT)$ is the sum-over-states, or "partition function," and g_i is the a priori probability, or "statistical weight," of the states. The net rate of energy absorption per unit volume by an average molecule is, then,

$$P = \frac{g}{Z}\left(w_i^j e^{-\overline{W_i^j}/kT} - w_j^i e^{-\overline{W_i^j}/kT}\right)\hbar\omega_i^j , \qquad (23)$$

where both states are assumed to have the same statistical weight g. The transition probability per unit time w_j^i accounts for induced emission from the excited states, emission which is coherent with the incident microwave. We neglect here spontaneous emission, since, as shall be emphasized later, this phenomenon is wholly negligible at microwave frequencies. Furthermore, at microwave frequencies $\hbar\omega/kT \ll 1$, since $kT/h \sim 6\times10^3$ kmc at room temperature. Expression (23) may be reduced approximately to

$$P \approx w_i^j \frac{(\hbar\omega_i^j)^2}{kT}\frac{g e}{Z}^{-\overline{W_i^j}/kT} . \qquad (24)$$

$\overline{W_i^j}$ is the average energy of the two states involved in the transition.

The absorption cross section at resonance is obtained now by combining (22) and (24):

$$\sigma(\omega_0) \equiv \frac{P}{\int I(\omega)d\omega} = \frac{4\pi(\omega_0^j)^2|\mu_i^j|^2 g e}{cKT\Delta\omega Z}^{-\overline{W_i^j}/kT} . \qquad (25)$$

Finally, the line "intensity," or maximum linear absorption coefficient

is given by

$$\gamma_0 \equiv N\sigma(\omega_0) = \frac{8\pi^2(\nu_{ij})^2|\mu_{ij}|^2 g}{cRT\Delta\nu Z} e^{-\bar{W}_i'/kT} \quad (cm^{-1}) \,, \tag{26}$$

where N is the number of molecules per unit volume. $\nu_{ij} \equiv \frac{\omega_{ij}}{2\pi}$ and $\Delta\nu \equiv \frac{\Delta\omega}{2\pi}$, the "line-breadth parameter," are substituted for computational convenience.

B. Causes of Line Breadth.

As is apparent in (26), the line-breadth parameter is an important factor in determining the intensity of an absorption line. There are a number of causes which broaden an absorption line[14,15,3]:

1. Natural line breadth.

The natural breadth of an absorption line is due to the finite lifetimes of the states involved. The average lifetimes of stationary rotational states of an unperturbed molecule are exceedingly long compared with those of electronic states; consequently, the spontaneous transition probability per unit time and hence the natural line breadth are very small. For microwave X-band frequencies (near 9 kmc) $\Delta\nu \sim 10^{-10}$ cps and is, therefore, wholly negligible.*

2. Doppler Broadening.

The random motion of molecules in a gas at temperature T gives rise to a Doppler shift which on the average broadens the absorption

---

* W. Heitler, reference 14, page 107.

line. The half-intensity, half-breadth is given by*

$$\Delta\nu = \frac{1}{2}\nu_0 \sqrt{\frac{2kT}{mc^2}\ln 2} = 3.6\times10^{-7}\nu_0\sqrt{\frac{T}{M}} \qquad (27)$$

where m is the molecular mass and M is the molecular weight in atomic weight units. For methyl chloride (CH_3Cl) at room temperature $\Delta\nu \sim 9$ kc.

3. Saturation broadening.

As we have seen in section A above the net absorption of microwave energy is possible because of the slight difference in the Boltzmann factors weighting the two states. For levels separated by X-band energies, the population of the initial level is only approximately 0.15% ($\sim h\nu/kT$) greater than that of the final level.

Even this small difference in populations becomes increasingly smaller as the level of the incident microwave power density increases. As a consequence the molecules are raised to an excited state at a rate comparable to that with which they are relaxed to their initial state. The overall effect is to decrease the absorption coefficient and to broaden the line.

The rate of relaxation of the molecules from excited states is determined primarily by intermolecular collisions, so saturation effects become significant when the incident microwave power

---

* W. Heitler, reference 14, page 116, equation (20b).

density exceeds the collision relaxation power per unit volume given by $P \approx \frac{N(h\nu)^2}{2kT}\bar{f}$, where $\bar{f}$ is the mean collision frequency.(16)

4. External-field broadening.

The breadth of Stark-or Zeeman-split lines due to stray or applied electric or magnetic fields is dependent in part on field homogeneity. For the case (discussed in section II-B) of symmetric-top molecules in a nearly uniform, static electric field it is clear from equation (18) that, for the first order effect, a field inhomogeneity $\Delta E/E$ will give rise to a line breadth of the order of

$$\Delta\nu = \nu\frac{\Delta E}{E} . \qquad (28)$$

Since in the case of direct transitions between rotational sub-levels the line is completely dependent on the static field for its existence, the requirements on field homogeneity are much more severe than for the usual case of $\Delta M = 0$ transitions.

5. Collision broadening.

Intermolecular collisions are a most significant cause of absorption line broadening for gas pressures greater than about 10^{-1} mm of Hg. At lower pressures, when the mean free path in the gas is comparable to the absorption cell dimensions, collisions with cell walls become important, too. In either case, the collision perturbations reduce the lifetime of excited states and hence

broaden the absorption line. At atmospheric pressure, for instance, the mean collision rates are of the order of 10^{10} collisions per second which means line half-breadths of at least 1.5 kmc -- usually considerably more for highly polar molecules. For lines centered in the X-band ($\sim$ 9 kmc), line breadths of this order are an appreciable fraction of the resonance frequency.

C. Absorption Lines Broadened by Collisions.

Since, except at fairly low pressures, collision broadening of microwave absorption lines is the dominant cause of line breadth, we need to consider this factor in more detail. On the assumption that the collision time is short with respect to the period of the microwave, an approximate expression for the absorption coefficient has been derived on semi-classical grounds by Van Vleck and Weisskopf[17]; particularized for Stark lines, it has the form

$$\gamma = \frac{4\pi^3 N\nu}{cKT} \sum_i \sum_j |\mu_{ij}|^2 \nu_{ij} f(\nu_{ij}, \nu) \frac{gc}{Z} e^{-W_i/KT}, \qquad (29)$$

where

$$f(\nu_{ij}, \nu) \equiv \frac{\nu}{\pi\nu_{ij}} \left[\frac{\Delta\nu}{(\nu_{ij}-\nu)^2 + (\Delta\nu)^2} + \frac{\Delta\nu}{(\nu_{ij}+\nu)^2 + (\Delta\nu)^2} \right]$$

is the "line-shape factor."

For the absorptive transitions between sublevels of a symmetric-top

molecule described in subsection II-B-2, the squared dipole matrix element as found by Reiche and Rademacher[18]* is

$$|\mu_i^{ij}|^2 \equiv |\mu_{JKM}^{JKM-1}|^2 = \mu^2 \frac{(J+M)(J-M+1)K^2}{4J^2(J+1)^2} \quad . \tag{30}$$

The statistical weight factor g generally is composed of the product of two factors; that is,

$$g = g_J g_I \quad . \tag{31}$$

In the present instance, the (2J + 1)-fold degeneracy of the energy levels with respect to J is removed by the electric field**; i.e., the statistical weight $g_J = 1$. For the important case of a symmetric-top molecule with a 3-fold symmetry axis, that is, three identical, symmetrically disposed atoms (NH_3, CH_3Cl, PF_3, etc.), the second statistical weight factor as calculated by Dennison[20] is

$$g_I = \tfrac{1}{3}(2I+1)(4I^2+4I+3) \qquad \text{for K divisible by 3, including 0;}$$

or (32)

$$g_I = \tfrac{1}{3}(2I+1)(4I^2+4I) \qquad \text{for K not divisible by 3.}$$

I is the nuclear spin of each of the identical nuclei. At room temperature kT is so small, compared with the energies of excited electronic

---

* Cf. D. M. Dennison, reference 19.

** The 2-fold degeneracy with respect to K remains.

states, that significant contributions to the partition function are made only by the vibrational and the rotational energies of the molecule. Interaction energies may be neglected at room temperature; then, for a perfect gas,*

$$Z = Z_{vib}\, Z_{rot} \,, \tag{33}$$

where

$$Z_{vib} \approx \prod_s \left(1 - e^{-hc\bar{\nu}_s/kT}\right)^{-d_s} . \tag{34}$$

$\bar{\nu}_s$ is a characteristic vibrational frequency of the molecule in cm^{-1} for a mode of degeneracy d_s. Also

$$Z_{rot} \approx \frac{(2I+1)^3}{3}\left[\frac{\pi}{B^3A}\left(\frac{kT}{hc}\right)^3\right]^{\frac{1}{2}} = \frac{56.2\,(2I+1)^3\,T^{\frac{3}{2}}}{B(kmc)\,[A(kmc)]^{\frac{1}{2}}} \tag{35}$$

for the symmetric-top with a 3-fold symmetry axis.

Finally, the average energy of the i and j states is given by

$$\overline{W_{ij}^{v}} = \frac{1}{2}\left(W_i + W_j\right) + hc\nu\bar{\nu}_s \,, \tag{36}$$

where W_i and W_j are the rotational energies calculated in part II. The vibrational quantum number v does not change during a microwave transition.

---

* G. Herzberg, reference 5, pp. 503, 506.

D. Pressure Dependence.

There are two factors in (29) which depend directly on the pressure of the gas, namely, the molecular density and the line-shape factor.

For the molecular density we may substitute its perfect-gas value given by

$$N = \frac{p}{kT} \quad . \tag{37}$$

If $\bar{f}$ is the mean collision frequency*, i.e., the mean number of effective collisions per second which induce a transition of the excited molecule to its initial state, then the half-breadth of a line involving the excited state will be

$$\Delta\nu = \frac{\bar{f}}{2\pi} \quad . \tag{38}$$

The mean collision frequency is, of course, related to the pressure. If it is assumed that the dependence is that given in the kinetic theory of gases,

$$\bar{f} \equiv \frac{\text{av. velocity}}{\text{mean free path}} = \frac{2\sqrt{\frac{2n_A kT}{\pi M}}}{\frac{1}{\sigma_c N}} = 2\sqrt{\frac{2n_A}{\pi RTM}}\,\sigma_c p \quad . \tag{39}$$

n_A is Avogadro's number, M is molecular weight in atomic mass units, and σ_c is the effective collision cross section. Combining (38) and (39) gives, finally,

$$\Delta\nu = \sqrt{\frac{2n_A}{\pi^3 RTM}}\,\sigma_c p \quad . \tag{40}$$

---

* $\bar{f}$ is the reciprocal of the mean effective collision interval.

The line-breadth parameter is found in this way to be proportional to the gas pressure.

The effect of pressure on the absorption coefficient of a single line as given by the Van Vleck-Weisskopf formula (29) may be considered as follows:

1. Narrow-breadth lines: $(\Delta\nu)^2 << \nu^2$

The line-shape factor reduces near resonance to

$$f(\nu_i, \nu) \approx \frac{1}{\pi}\left[\frac{\Delta\nu}{(\nu_i - \nu)^2 + (\Delta\nu)^2}\right], \tag{41}$$

which for resonance becomes simply

$$f(\nu_i, \nu) \approx \frac{1}{\pi\Delta\nu}. \tag{42}$$

Expression (29) gives for a single line

$$\gamma_0 \approx \frac{8\pi^3 N\nu^2 |\mu_i^j|^2 g e^{-\overline{W}_i^j/kT}}{ckT\Delta\nu Z}, \tag{43}$$

which is precisely equation (26) derived in section A above.

Now, since N and $\Delta\nu$ vary linearly with pressure, one finds by substituting (37) and (40) in (43) that

$$\gamma_0 \approx \frac{4}{c}\sqrt{\frac{2\pi^7}{\eta_4 k^3}} \frac{\nu^2 |\mu_i^j|^2 g}{Z\sigma} e^{-\overline{W}_i^j/kT} \sqrt{\frac{M}{T^3}}. \tag{44}$$

The maximum absorption coefficient evidently is independent of gas pressure, a law which holds over a pressure range approximately 10^{-1} to 10^2 mm of Hg.*

---

* W. Gordy, reference 3, page 705.

If one considers the possibility of pressure so low that collision broadening ceases to be the dominant factor in determining $\Delta\nu'$, then expression (43) indicates that the absorption coefficient falls off as the molecular density, or pressure, is decreased.

2. Medium-breadth lines: $(\Delta\nu')^2 \sim \nu'^2$

All terms must be retained in the line-shape factor for this intermediate case. The maximum absorption coefficient is no longer independent of gas pressure, but appears to increase gradually with increasing pressure, and further, to shift to lower frequencies.

3. Wide-breadth lines: $(\Delta\nu')^2 >> \nu'^2$

The line-shape factor reduces to a form similar to Debye's expression for non-resonant dispersion*:

$$f \approx \frac{2}{\Delta\nu'} \frac{1}{1+\left(\frac{2\nu'}{\Delta\nu'}\right)^2} \quad . \tag{45}$$

---

* P. Debye, reference 4, page 90; Cf. V. H. Van Vleck, reference 21.

IV. A NEW MICROWAVE STARK-EFFECT SPECTROMETER

A complete spectrometer has been designed and built especially for an exploratory investigation of the direct absorptive transitions between rotational sublevels of symmetric-top molecules in orthogonal fields. The heart of the device is, of course, the absorption cell which confines the test gas to a region of static and microwave electric fields. In addition, a microwave signal source, transmission and detection system are requisite. The design of the spectrometer entailed consideration of a number of interrelated factors.

A. Some Design Considerations

In section B of part II, it was stressed that direct transitions are allowed only when the microwave electric vector is, or has a component, parallel to the static electric field. The Stark electrodes must necessarily, then, comprise part of the boundary containing the microwaves; since, while the static field is normal to the electrode surfaces, the microwave electric vector parallel thereto must be zero. Plane-parallel electrodes are indicated by the need for a uniform field to minimize field inhomogeneity broadening of the absorption line (see page 17). An insulating gap, furthermore, must separate the electrodes from each other and from the rest of the boundary. It is desirable, although not essential, to avoid a design which allows eddy currents to circulate with a component normal to the gap.

1. Resonant cavity

A design which fulfills all the foregoing requirements is illustrated in Figure 7: a right circular cylinder excited in the TE_{01p} mode so that the microwave electric vector is everywhere perpendicular to the static electric field established between the plane ends of the cavity. Since the microwave electric field is, moreover, everywhere circularly solenoidal, no eddy currents flow in the walls normal to the gaps between the electrodes and the cavity cylinder. While resonant cavities have been used before[22] as absorption cells, the writer believes that the Stark-splitting cell to be described here is original.

In a general way, the longer the path of the microwave through the test gas, the greater the absorption effect. While one might less conveniently employ a long length of wave guide for an absorption cell as is commonly done, it is apparent that for compactness and simplicity the resonant cavity is superior -- if broad-banding is not essential. It is easily shown (see section C, part V) that a wave guide to be equally as effective as a transmission cavity having a loaded quality factor Q_o' would have to have an effective length* of the order of

$$L_{eff} \sim \frac{2Q_o'}{\beta} \quad , \tag{46}$$

where $\beta \equiv \frac{\omega}{c}$, c being the phase velocity of the microwave in free space. For X-band microwaves and for a reasonable value of Q_o' ,

---

* Somewhat longer than the physical length of the wave guide.

the effective length would be of the order of 30 meters or more. That a cavity only a few centimeters long can be as effective an absorption cell as a very long wave guide is not surprising when one considers the thousands of wave reflections over the same path in the cavity.

2. Cavity characteristic frequency and Stark voltage

A resonant-cavity absorption cell having been chosen, the next consideration is the choice of a characteristic frequency. This frequency is the ν of the incident radiation discussed in part III above. The cavity should, first of all, resonate at the frequency of the absorption line to be investigated:

$$\nu_{JKM}^{JKM-1} = \frac{\mu E}{h} \frac{K}{J(J+1)} \quad . \qquad (18)$$

Now, the lowest TE_{01p} mode, p = 1, of the cavity has a characteristic frequency given by (see page 32)

$$\nu_o = \left[\left(\frac{c}{2d}\right)^2 + \nu_c^2\right]^{\frac{1}{2}} , \qquad (47)$$

where ν_c is the cutoff frequency.

The desirability of keeping the electrode voltage as low as possible will soon be apparent. To further this end, clearly, as small as possible a value of electrode spacing is to be sought; so a cavity design should be chosen such that $\nu_c << \frac{c}{2d}$, in which case

$$\nu_o \approx \frac{c}{2d} \quad . \qquad (48)$$

Solving for the interelectrode spacing d from (48) and for the static

electric field E from the above expression for the line frequency gives for the voltage to be applied to the electrodes

$$V = Ed \simeq \frac{ch}{2\mu} \frac{J(J+1)}{K} \quad . \tag{49}$$

The Stark voltage for resonance evidently is independent of frequency and depends principally on the dipole moment and the rotational level being split. For a dipole moment $\mu = 1$ Debye (10^{-18} esu) and for the lowest permissible rotational state $J = K = 1$, $V \approx 200$ esu $= 60{,}000$ volts! It is apparent that independent of the frequency, an inordinately high voltage must be applied across the absorption cell.

The question of cavity characteristic frequency is still undecided, however. Let us examine in general terms the dependence of microwave absorption on frequency. First of all, note that in (29) the maximum absorption coefficient, that is, the absorption of radiation in nepers per unit path length, increases explicitly as ν_o^2. As is implicit in (46) the total path length increases approximately with $\nu_o^{-\frac{3}{2}}$, taking into account the $\nu_o^{-\frac{1}{2}}$ dependence of Q_o'. Thus, for a given absorption line, the overall absorption seems to increase roughly as $\nu_o^{\frac{1}{2}}$, which result favors the choice of a high frequency.

There is an additional consideration of significance, namely, the dielectric strength of the gas under test. It was found above that the voltage across the plane-parallel electrodes is essentially

fixed for a given absorption line. By Paschen's law[23], then,

$$(pd)_{min} = \text{constant}, \tag{50}$$

where p is the gas pressure and d is the interelectrode spacing. For narrow-breadth lines (page 22), this restriction implies

$$d_{min} \propto \frac{1}{\Delta\nu} ;$$

which, in view of (48), means

$$(V_0)_{max} \propto \Delta\nu , \tag{51}$$

Hence, if excessive collision broadening of the absorption line is to be avoided, the frequency must not be too high.

In conclusion, it appears that over the range of microwave frequencies convenient for this type of experiment, say 3000 mc to 30,000 mc, there is only a factor of about 3 in the overall absorption of a given line. If one chooses to go to frequencies below the microwave region in order to reduce the line-breadth parameter, he is faced with giving up the resonant cavity and the long effective absorption path it provides, as well as a lower absorption coefficient. For the foregoing reasons and in consideration of convenience, it was decided to conduct an exploratory investigation in the X-band.

3. Absorption-cell septum

To avoid excessive broadening of the absorption line by static field inhomogeneity, it is clearly desirable to confine the gas under test to the central region of nearly uniform field between the Stark electrodes. To withstand the relatively intense fields in the re-

gions of the gaps between the electrodes and the cylinder, the gas would have to be maintained at a very high pressure indeed, a condition which would surely give rise to excessive collision broadening.

An absorption cell boundary, then, is to be sought which (a) does not alter appreciably the static field inside the cell, (b) perturbs the microwave field as little as possible, and (c) has sufficient mechanical rigidity and vacuum seal to contain the gas.

Requirement (a) is readily met by an open-end tubular dielectric septum closed by the plane-parallel electrodes. Satisfaction of requirement (c), however, seriously conflicts with requirement (b). That is, a septum which is large enough to meet constructional requirements, appreciably affects the characteristic frequency of the cavity. In view of the relatively narrow tuning range ($\sim$17%) of the microwave signal source it is necessary to be able to choose the cavity and the septum dimensions so that the characteristic frequency of the combination falls within tuning range.

The idealized geometry of the system to be considered is illustrated in Figure 8. For simplicity the narrow annular gaps between the electrodes and the cylinder are neglected. The tube of dielectric constant K is positioned coaxially with respect to the cylindrical wall of the cavity. To obtain the characteristic frequencies of the system, one must apply the appropriate boundary condition to solutions of the homogenious wave equation in the three regions indicated:

$$\nabla^2 W + \beta'^2 W = 0 \,, \qquad (52)$$

where $\beta'^2 \equiv \frac{\omega^2}{v_p^2}$, v_p being the appropriate phase velocity. If we let the wave function[24]

$$W = U(\rho,\varphi) Z(z) , \tag{53}$$

equation (52) separates into

$$\nabla_2^2 U(\rho,\varphi) + \beta_{mn}^2 U(\rho,\varphi) = 0 \tag{54}$$

and

$$\frac{d^2 Z(z)}{dz^2} + (\beta'^2 - \beta_{mn}^2) Z(z) = 0 \tag{55}$$

where β_{mn}^2 is a separation constant. An obvious choice for Z(z) is

$$Z(z) = \sin \frac{p^2\pi^2}{d^2} , \quad p = 1,2,3, \cdots . \tag{56}$$

The eigenvalues of d^2/dz^2 which belong to Z(z) are clearly given by

$$\beta_{mnp}'^2 - \beta_{mn}^2 = \frac{p^2\pi^2}{d^2} , \tag{57}$$

from which the characteristic frequencies are

$$\omega_{mnp}^2 = v_p^2 \beta_{mnp}'^2 = v_p^2 (\beta_{mn}^2 + \frac{p^2\pi^2}{d^2}) . \tag{58}$$

Our next task is to find the eigenvalues β_{mn}^2 of the two-dimensional Laplacian ∇_2^2 which belong to $U(\rho,\varphi)$. An appropriate solution of (54) is

$$U(\rho,\varphi) = [A J_m(\beta_{mn}\rho) + B Y_m(\beta_{mn}\rho)] \cos m\varphi , \tag{59}$$

where $J_m(\beta_{mn}\rho)$ and $Y_m(\beta_{mn}\rho)$ are Bessel functions of the first and second kind.

Since only the symmetric modes TE_{01p} are of interest here, set m = 0 and n = 1 and choose

$$U_1 = A_1 J_0(\beta_1 \rho) \qquad \text{in region 1,}$$

$$U_2 = A_2 J_0(\beta_2 \rho) + B_2 Y_0(\beta_2 \rho) \qquad \text{in region 2,} \tag{60}$$

and

$$U_3 = A_3 J_0(\beta_1 \rho) + B_3 Y_0(\beta_1 \rho) \qquad \text{in region 3,}$$

where $\beta_1^2 \equiv \frac{\omega_{01p}^2}{c^2} - \frac{p^2\pi^2}{d^2}$ and $\beta_2^2 \equiv \frac{K\omega_{01p}^2}{c^2} - \frac{p^2\pi^2}{d^2}$ from (58)*.

Applying the boundary conditions which require continuity of $E_\varphi = \frac{j\omega}{c} \frac{\partial \bar{W}}{\partial \rho}$ and $H_z = \beta_{mn}^2 \bar{W}$ at each surface, one obtains a determinantal equation**

$$\begin{aligned} &[\eta S_{11}(s,\xi) S_{01}(r,\eta) - s\xi S_{10}(s,\xi) S_{11}(r,\eta)] s\xi J_0(r s\xi) \\ &-[\eta S_{11}(s,\xi) S_{00}(r,\eta) - s\xi S_{10}(s,\xi) S_{10}(r,\eta)][\eta J_1(r s\xi)] = 0 \end{aligned} \tag{61}$$

where for convenience $\eta \equiv \beta_2 b_2$, $\xi \equiv \beta_1 a$, $r \equiv \frac{b_1}{b_2}$, $s \equiv \frac{b_2}{a}$

and $S_{kl}(x,y) \equiv J_k(y) Y_l(xy) - J_l(xy) Y_k(y)$.

For purposes of computation it is well to expand (61) in terms of a small septum-thickness parameter defined as $\delta \equiv 1 - r \equiv b_2 - b_1 / b_2$.

---

* The mode designation m, n = 0, 1 is dropped for brevity.

** From a 5th order determinant.

After a somewhat lengthy calculation one finds

$$\sum_k \sum_\ell \frac{\delta^{k+\ell}}{k!\ell!}\left(1-\frac{\delta}{2}\right)^{k+\ell}\Big\{(\xi\xi')^{\ell+1}\eta^{k-1}J_\ell(\xi\xi')\left[\xi\xi'_{11}(\xi,\xi')R_{k,1}(\eta)-\xi\xi'_{10}(\xi,\xi')R_{k-1,2}(\eta)\right]$$

$$-(\xi\xi')^{k}\eta^{\ell}J_{k+1}(\xi\xi')\left[\eta\xi'_{11}(\xi,\xi')R_{\ell-1,1}(\eta)-\xi\xi'_{10}(\xi,\xi')R_{\ell-2,2}(\eta)\right]\Big\}=0\ , \tag{62}$$

where the $R_{mn}(\eta)$ are Lommel polynomials given by

$$R_{mn}(\eta)\equiv\left[J_{m+n}(\eta)Y_{m-1}(\eta)-Y_{m+n}(\eta)J_{m-1}(\eta)\right]\frac{\pi\eta}{2}\ .$$

The first order term in δ is readily found from (62):

$$J_1(\xi)=-\frac{\pi}{2}\delta(K-1)(\xi^2\xi'^2+\gamma^2)J_1(\xi\xi')\xi'_{11}(\xi,\xi')+O(\delta^2)\ \text{etc.}, \tag{63}$$

in which $\gamma^2\equiv\rho^2\pi^2/(b_2)^2$.

Equation (63) is solved graphically for ξ, the desired eigenvalues β_1 times a ; so finally the characteristic frequencies of the cavity are given by

$$\nu_0=\left[\left(\frac{\rho c}{2d}\right)^2+\nu_c^2\right]^{\frac{1}{2}} \tag{64}$$

from expression (58), where $\nu_c\equiv\frac{c}{2\pi}\beta_1\equiv\frac{c\xi}{2\pi a}$.

In the absence of the septum, i.e., for $\delta=0$, (63) gives simply

$$J_1(\xi)=0\ . \tag{65}$$

For p = 1 we use the first root of equation (65); namely, $\xi_1=3.83$.

The microwave electric field is for this limiting case

$$E_\varphi=AJ_1\left(\xi_1\frac{\rho}{a}\right) \tag{66}$$

and

$$E_\rho=E_z=0\ .$$

B. Cavity Construction

In view of the considerations discussed in section A, a design for a resonant-cavity absorption cell was evolved and a prototype was constructed. Figure 9 is a photograph of the resonant-cavity assembly showing the cavity cylinder and its means of support.

With the cylinder removed, the absorption-cell assembly is visible in Figure 10. The Stark electrodes (a), mounted on lucite insulators, form the ends of the resonant cavity. Clamped between the electrodes is the tubular septum (b) which confines the test gas to the axial region where nearly uniform static field obtains. The cylinder shown in Figure 9 is spaced from the elctrodes by small annular gaps and is at ground potential.

1. Cavity finish.

The electrodes, machined from brass rod stock, are painstakingly lapped to a high degree of planarity. To grade the electric field in the gap, a radius is machined on the electrode edges. First copper plated, then gold plated, the electrodes and cavity cylinder are carefully polished in order to insure a high quality factor for the cavity. We shall see later that the spectrometer sensitivity is proportional to the unloaded Q.

2. Coupling loops.

Small wire loops (c) diametrically positioned serve to transmit microwave energy into and out of the cavity. The plane of the loops is parallel to the end planes of the cavity and midway between so that the TE_{011} mode (p = 1) is excited. The loops are mounted

so that radial adjustment is provided, by means of which the coupling parameter (see part V) can be varied.

3. Septum.

A considerable amount of time was spent in developing a suitable practical design for the dielectric septum. Dupont's Teflon (polymerized C_2F_4) is a material most satisfactory for the purpose, since it has a low power factor (0.0002 at 9 kmc), low dielectric constant ($K = 2.0$), zero permanent dipole moment, high surface resistance, and good machineability.

The outer radius b_2 (Figure 8) of the tube is chosen as large as possible in order to include as much of the strong microwave field (see Figure 7) as possible, but not so large as to extend into the gap-field fringe. The axial dimension d and the inner radius b_1, are then selected in accord with equations (63) and (64) for a particular characteristic frequency.

Several Teflon septa were machined in the course of the investigation. Remarkably good agreement was obtained between theoretical and experimental characteristic frequencies. Table 1 lists some of the results. The value of b_2 fixed upon places the septum in the region of microwave field about 67% of maximum intensity, which means that the influence of the dielectric piece on the characteristic frequency is considerable. If, in fact, the thickness parameter δ is increased only slightly above the value listed, the fundamental characteristic frequency jumps from values below to values <u>above</u> the characteristic frequency of the cavity without the septum in place.

One further problem with respect to the septum must be mentioned here, that is, the vacuum seal between the dielectric tube and the plane-parallel electrodes.

The first solution tried was to machine a small groove in each end of the Teflon tube, in which were placed two 1/16 inch rubber O-rings. Since commercial O-rings of this small cross section are not available in sufficiently large diameters, it was necessary to vulcanize rings from Buna-N rubber string stock. Properly treated with high-vacuum grease, these O-rings provide excellent vacuum seals. Unfortunately, however, an appreciable decrease in the Q of the cavity resulted from the introduction of this relatively lossy material, even though the rings are in regions of very low electric field.

The last difficulty was circumvented finally by discarding the rubber O-rings in favor of a "Teflon O-ring": a 0.050 inch radius machined and polished on each end of the tube. Teflon is sufficiently elastic so that when the tube is squeezed between the electrodes a total of about 0.004 inch, a satisfactory vacuum seal is obtained.

4. Adjustment

Spring-loaded cap-nuts (d) provide for adjustment of the Stark electrodes to a degree of parallelism of the order of 100 microinches measured at peripheral points diametrically opposite. It is by means of these cap-nuts that the septum is sealed in place.

Stud-nuts (e) serve to position the cylinder so that its axis is normal to the electrodes and so that the plane of the coupling loops is midway between the electrodes.

5. Gas duct.

The test gas is introduced into the axial region inside the Teflon septum through a small hole in the lower electrode which is fed by lucite duct (f).

C. High-Voltage Insulation and Allied Problems.

Since voltages up to 60 kv are applied across the Stark electrodes, the problem of providing sufficient insulation is a difficult one. The annular gap separating the electrodes from the cavity cylinder is only 0.150 inch wide while the electrodes are separated by 0.654 inch. Not only is sparkover to be avoided, but some means is needed to suppress corona; for excessive corona noise would seriously reduce the ultimate sensitivity of the spectrometer (see part V).

The possibilities of solid dielectrics and of nitrogen, Freon, etc. under pressure for insulation were weighed. The solution finally adopted, however, was to evacuate the air from around the entire cavity assembly. This course proved to be a wise one, since external corona noise was found to be appreciable.

The high-voltage buses enter the evacuated region through vacuum bushings (g), while the microwave lines pass through the pump table by means of vacuum coaxial bushings (h).

Figure 11 is a schematic diagram of the vacuum system employed. By means of an oil diffusion pump and a Megavac forepump a vacuum of 10^{-4} to 10^{-5} mm of Hg. was obtained in the bell jar surrounding the cavity. An O-ring (Figure 9) was a most effective vacuum seal between the bell jar and the pump table. Countless hours of waxing on the jar in the "classical" manner were thereby saved.

Of considerable convenience in leak hunting and in indicating when to turn on the diffusion pump was the pirani gauge shown in Figure 11.

Further to increase the surface resistance of the Teflon septum a very fine (224 threads per inch) thread was chased on the inner cylindrical wall of the piece.[25] Before this step was taken surface arc-over was prevalent.

D. Test-Gas Injection System.

The system devised to inject a small quantity of the gas under test into the absorption cell is also shown in Figure 11. High-vacuum cocks are so arranged that the absorption cell can be switched to the high-vacuum system described above. A Hyvac pump evacuates the air from the outer vacuum plumbing, which is then filled with gas for injection. Finally, the absorption line is turned from the high vacuum to let in a gas specimen. The entire system is, of course, flushed out several times before the test sample is retained.

To insure that the gas is thoroughly dry, it is allowed to remain several minutes in contact with a perchlorate or sulphate drier before it is passed on for use.

A bourdon-type vacuum-pressure gauge and a coaxial mercury manometer are used to measure the gas pressure.

E. High-Voltage Supply and Metering.

To provide the 0-60 kv needed for Stark splitting, a 0-30 kv doubler was engineered and constructed. The device is required to supply only several milliamperes for metering purposes and leakage losses.

Figure 12 is a schematic diagram of the supply and Figure 13 shows the device as it was built. The positive voltage is applied to one electrode, while the equal negative voltage is connected to the other. Three-megohm sparkover suppressors are inserted in series with each lead.

Calibrated 0-1 ma. meters in conjunction with two multipliers, each consisting of thirty 1 megohm precision resistors ($\frac{1}{2}\%$), are used to measure the voltage applied to the Stark electrodes. The static electric field E, then, is calculated by dividing the sum of the voltages by the interelectrode spacing as measured with a micrometer.

F. Microwave Plumbing.

The absorption-cell cavity is placed in one arm of a differencing bridge as shown in Figure 14. This arrangement not only prevents overloading the detection amplifiers, but also cancels out some of the instabilities in the signal source.

An X-band reflex klystron (723A/B) provides the source of microwave energy. This oscillator supplies at the most 20-30 milliwatts of r-f power over the frequency range 8.4 to 9.6 kmc. A 1 kc square-wave voltage is applied through a cathode-follower modulator to the klystron reflector so as effectively to switch the oscillator in and out of oscillation. This widely used technique, similar to the beam choppers employed in infrared spectrometers, allows the use of a-c amplifiers in detection.

The microwave output of the klystron oscillator, after passing through a pad attenuator, is divided; part is fed to the cavity through a coaxial cable, the rest passes through a variable attenuator for differencing purposes and is detected by a silicon crystal.

The cavity output pickup loop is coupled in turn through a coaxial cable to an isolating pad attenuator, a standing wave-meter, a variable-stub tuner, and a IN26 silicon crystal for detection. Considerably more stable than the IN23B, the IN26, a K-band (30 kmc) video crystal, was found to be most satisfactory. A special mount had to be devised to accommodate the coaxial crystal in the cartridge-type crystal holder.

G. Detection and Recording System.

1. Differencing amplifier.

The square-wave voltages from the two crystal detectors are fed into a differencing amplifier, so that only the change in the signal through the cavity which results from absorption of microwave energy in the gas is passed on for recording. Figure 14 is a block diagram of the system while some of the details of circuitry are shown in Figure 15.*

2. Narrow-band amplifiers.

A narrow-band amplifier employing parallel-T filters tuned to 1 kc follows the differencing amplifier and serves to reject an appreciable amount of thermal and shot noise from the crystals and the first tube. Only the fundamental sine wave from the difference signal is passed on to balanced lock-in amplifiers for detection.

3. Balanced lock-in amplifiers.

This type of detector was first suggested by R. H. Dicke[26,27]. A lock-in amplifier is essentially a zero-frequency heterodyning

---

* Regulated power supplies are not shown.

system by which a very weak signal in the presence of excessive narrow-band noise is beat against a strong coherent signal of the same frequency.* The resultant zero-frequency, or d-c, component is passed through a low-pass filter to reject much of the noise.

In the present scheme, two lock-in amplifiers are arranged in a balanced fashion in order to cancel out strong spurious impulses which originate in the test gas when it is subjected to the high static electric fields. These "Geiger-counts" were a serious source of interference before the balanced system was devised. Two type 5693 Red tubes are used as pentode converters: the weak signal is fed onto the control grids while the heterodyne signal drives the suppressor grids 180° out of phase with respect to one another.

4. Phase-shifter and phase-splitter.

Maximum signal-to-noise ratio obtains in the output of the lock-in amplifier when the heterodyning voltage is either in phase or 180° out of phase with the weak signal to be detected. The heterodyne signal is obtained from the modulation source (see Figure 14) and is passed through a phase-shift network and a phase-splitter to the suppressor grids of the lock-in amplifier. The phase-splitter provides two signals 180° out of phase for application to the suppressor grids of the lock-in amplifier pentodes.

5. Low-pass filter.

A double-pi RC ladder-net having a time constant of about two seconds serves as a low-pass filter to reject the unwanted noise, while passing the d-c component from the converter which is proportional to the difference signal.

---

* Cf. C. A. Stutt, reference 28, for a theoretical treatment.

6. Balanced d-c amplifier.

Following the low-pass filter is a pair of type 5693 triodes arranged to take the difference of the d-c signals from the two lock-in amplifiers. A Helipot fine balancing control is incorporated in the plate circuit.

7. Brush amplifier and recorder.

Finally, the signal from the balanced d-c amplifier is fed into a Brush Corp. amplifier for further amplification. A decade attenuator in the input circuit is used for calibration purposes to be described later.

The amplifier drives in turn one pen-motor of a dual-channel Brush recorder. Proportional to the difference signal, which varies linearly with the microwave power absorbed by the gas in the absorption cell, the pen deflection is a measure of the absorption coefficient of the gas.

To provide for recorded correlation of the absorption coefficient with the associated Stark voltage, the second channel of the recorder is fed, through another amplifier, with a voltage proportional to the high voltage applied to one of the Stark electrodes. A permanent record of the absorption coefficient versus Stark voltage is thereby obtained.

The equipment described above is shown in Figure 16, a photograph of the assembled microwave Stark-effect spectrometer.

V. SPECTROMETER SENSITIVITY

It is appropriate to inquire next into the factors governing the sensitivity of the spectrometer described in part IV. For purposes of adjustment and calibration, as well as design, it is necessary to understand the elements which determine and limit the capability of the device for measuring the small attenuation of the microwaves in traversing the test gas.

A. Cavity Transmission and Sensitivity Factor.

Consider first the absorption-cell cavity and its transmission characteristics. Figure 17 is an equivalent circuit which applies approximately near a characteristic resonance to a high-Q cavity such as is employed, with particular reference planes for input and output circuits.[29]

The input and output lines are considered to have the same real characteristic impedance, and to have, furthermore, equal couplings to the cavity. With these assumptions the power delivered to the output line is easily found to be

$$P_o = \frac{(KQ I_g)^2 / Z_o}{(1+2KQ)^2 + Q^2\left(\frac{\omega}{\omega_o} - \frac{\omega_o}{\omega}\right)^2}, \tag{67}$$

where a coupling parameter $K \equiv n^2 Z_o / \omega_o L$ is defined and where the unloaded quality factor is $Q \equiv \frac{\omega_o L}{R}$, $\omega_o \equiv \frac{1}{\sqrt{LC}}$.

The cavity transmission loss function is, then,

$$T(\omega) \equiv \frac{P_o}{P_a} = \frac{(2KQ)^2}{(1+2KQ)^2 + Q^2\left(\frac{\omega}{\omega_o} - \frac{\omega_o}{\omega}\right)^2}, \tag{68}$$

which is simply the output power divided by the available power $P_a \equiv V_g^2/4Z_o$. Since we are primarily interested in the transmission at resonance, we set $\omega = \omega_o$ to find the peak transmission:

$$T(\omega_o) = \frac{(2KQ)^2}{(1+2KQ)^2} \quad . \tag{69}$$

The next task is to relate the cavity Q to the absorption coefficient of the gas in the absorption cell. There are, of course, two principal sinks of energy represented by the lumped parameter R: (1) ohmic losses due to eddy currents in the cavity walls, and (2) microwave energy absorption in the gas. The Q factor of the cavity is defined as

$$Q \equiv \omega \frac{\text{energy stored}}{\text{rate of energy loss}} \quad . \tag{70}$$

The energy stored in the cavity is simply given by

$$\text{energy stored} = \int_{cav.} u\,dV \,, \tag{71}$$

where u is the microwave energy density. Also the

$$\text{rate of energy loss} = \frac{\omega}{Q_o}\int_{cav} u\,dV - \frac{\partial}{\partial t}\int_{cell} u\,dV \,, \tag{72}$$

Q_o being the quality factor for the cavity without the gas.

Bouquer's law defines the linear absorption coefficient in accord with

$$\frac{du}{dz} \equiv -\gamma u \,, \tag{73}$$

where z is the direction of the plane running waves which make up the standing wave in the cavity. Now it follows that

$$\frac{\partial u}{\partial t} = \frac{\partial u}{\partial z}\frac{dz}{dt} = -\gamma v_p u . \qquad (74)$$

v_p is the phase velocity of the microwave through the gas. Substituting (74) into (72), after commuting the time derivative and the space integral, gives the

$$\text{rate of energy loss} = \left[\frac{\omega}{Q_0} + \gamma v_p P\right]\int_{cav} u\,dV , \qquad (75)$$

where $P \equiv \int_{cell} u\,dV \Big/ \int_{cav} u\,dV$, an "absorption-cell space factor" is introduced.

The effective quality factor is obtained, finally, by inserting (71) and (75) in definition (70):

$$Q = \frac{Q_0}{1 + \frac{PQ_0\gamma}{\beta'}} , \qquad (76)$$

in which the phase constant $\beta' \equiv \omega/v_p$.

In many practical cases, γ is so small that an excellent approximation for (76) is

$$Q \approx Q_0\left(1 - \frac{PQ_0\gamma}{\beta'}\right) . \qquad (77)$$

Consequently, the decrement in Q caused by gas losses is

$$\Delta Q \equiv Q_0 - Q \approx \frac{PQ_0^2}{\beta'}\gamma . \qquad (78)$$

It is now convenient to calculate a cavity sensitivity factor S defined by

$$\Delta\Gamma(\omega) \equiv S\gamma , \qquad (79)$$

which relates the loss in cavity transmission due to a gas absorption

coefficient γ . Combining (78) and (79) yields

$$S = \frac{\ell Q_0^2 \Delta\Gamma}{\beta' \Delta\varphi} \quad . \tag{80}$$

The second term in the right member of equation (80) is easily evaluated from equation (69):

$$\frac{\Delta\Gamma}{\Delta\varphi} \approx \frac{d\Gamma}{d\varphi} = \frac{8K^2\varphi}{(1+2K\varphi)^3} \quad . \tag{81}$$

The cavity sensitivity factor is, finally, given by

$$S \approx \frac{8\ell K^2 Q_0^3}{\beta(1+2KQ_0)^3} \quad , \tag{82}$$

noting that $\varphi \approx Q_0$ and that $\beta' \approx \beta = \frac{\omega}{c}$.

Since the coupling parameter can readily be varied in the design described in part IV, we may find its optimum value by maximizing S:

$$\frac{dS}{dK} = 0$$

yields the simple value

$$K_{opt.} = \frac{1}{Q_0} \quad . \tag{83}$$

Substituting this optimum value of K in (82) and (69), one finds for maximum sensitivity

$$S = \frac{8}{27} \frac{\ell Q_0}{\beta} \quad , \tag{84}$$

and for the optimum transmission

$$\Gamma_{OPT} = \frac{4}{9} \cdot \tag{85}$$

Relation (85) provides a useful condition for adjusting the cavity coupling loops to optimum K.

B. Calibration Relation.

For purposes of calibrating the spectrometer the readily measured loaded quality factor Q_o' is a preferable parameter. By examination of the equivalent circuit of Figure 17, it is easily verified that

$$Q_o' = \frac{Q_o}{1+2KQ_o} \cdot \tag{86}$$

The maximum cavity sensitivity is, then,

$$S_{max} = \frac{8}{9} \frac{LQ_o'}{\beta}, \tag{87}$$

where $Q_o' = Q_o/3$ is the optimum loaded quality factor.

One procedure for calibrating the overall system is to change one of the calibrated attenuators in series with the cavity (see Figure 14) and to note the difference signal on the recorder. Suppose a convenient increment $\Delta\alpha$ (in db) in the attenuator setting causes a deflection of the recorder pen r units. Clearly, a fractional change in cavity transmission

$$\frac{\Delta\Gamma}{\Gamma} = 10^{\frac{\Delta\alpha}{10}} - 1 \tag{88}$$

will give rise to the same deflection. The absorption coefficient corre-

sponding to deflection r is

$$\gamma_r = \frac{\Gamma}{S'}\left(10^{\frac{\Delta\alpha}{10}} - 1\right) \quad . \tag{89}$$

For computation (85), (87), and $\beta = 2\pi\nu_0/c$ give

$$\frac{\Gamma}{S'} = \frac{\pi^2\nu_0}{cPQ_0'} \quad . \tag{90}$$

C. Equivalent Wave-guide Length.

In passing, it is interesting to note the appearance of the quantity Γ/S', which is simply the reciprocal effective length of an equivalent wave-guide absorption cell. To verify this contention consider the fractional change in transmission loss in a wave guide of effective length L_{eff} filled with gas of absorption coefficient γ. By Bouquer's law (73),

$$\frac{\Delta\Gamma}{\Gamma} \approx \gamma L_{eff} \, , \tag{91}$$

if $\gamma L_{eff} << 1$. Thus, in terms of cavity sensitivity given by definition (79)

$$L_{eff} \approx \frac{S'}{\Gamma} = \frac{2PQ_0'}{\beta} \quad . \tag{92}$$

The physical length of the wave guide is somewhat shorter, depending on how near to cut-off the guide is operated. The physical length is of the order of

$$L = \frac{\beta_g}{\beta} L_{eff} \approx \frac{2\beta_g}{\beta^2} PQ_0' \, , \tag{93}$$

where $\beta_g \equiv \omega/v_g$, $\beta \equiv \omega/c$. v_g and c are the phase velocities in the guide and in free space, respectively.

D. Ultimate Sensitivity of the Spectrometer.

To provide a rough estimate of the ultimate sensitivity, or minimum absorption coefficient which can be measured with a spectrometer of the type described, we consider as the limiting factor the thermal and the shot noise generated in the detection crystals and in the first tube of the differencing amplifier.* Each crystal may be regarded as a current source shunted by an internal audio resistance R_c.(30) The noise voltage at the input of the lock-in amplifier is, then,

$$V_n = G\left[4kT_0(2tR_c + R_a)\Delta f\right]^{\frac{1}{2}}, \qquad (94)$$

where t is the noise-temperature ratio of the crystal, $T_0 = 300^\circ K$, R_a is the equivalent noise resistance of the first tube**, G is the voltage gain of the differencing and parallel-T amplifiers and Δf is the noise band width.

Above approximately 30 mc the noise-temperature ratio t is nearly unity, while below several hundred kilocycles t increases inversely with frequency. Below 5 - 10 microwatts of incident microwave power, however, t is nearly independent of frequency.

In the square-law region the strength of the crystal current source is

$$i = \frac{P_i}{b}, \qquad (95)$$

where P_i is the incident microwave power and b is a crystal constant. The difference-signal output from the amplifier is evidently

$$V_s = GR_c\frac{\Delta P_i}{b}. \qquad (96)$$

---

* Cf. Gordy, reference 3, page 677.

** Referred, of course, to the input transformer primary circuit.

In accord with the usual criterion for detectability we take $V_s = V_m$, which gives

$$\Delta P_i = \frac{1}{M'}\left[4kT_o\Delta f\right]^{\frac{1}{2}}. \tag{97}$$

A modified crystal figure of merit is introduced for convenience; that is,

$$M' \equiv \frac{R_c}{b\sqrt{2tR_c+R_a}}.$$

The difference-power signal arising from gas losses in the cavity absorption cell is simply

$$\Delta P_i = \alpha P_a \Delta\Gamma = \alpha P_a S_{max}\gamma. \tag{98}$$

Here α is the transmission loss* from the cavity to the crystal. Equating (97) and (98) and solving for γ yields, finally,

$$\gamma_{min.} = \frac{\left[4kT_o\Delta f\right]^{\frac{1}{2}}}{M'\alpha S_{max}P_a} \tag{99}$$

as the minimum detectable absorption coefficient.

For example, assume reasonable values; such as, $t = 10$, $R_c = 2\times10^3\,\Omega$, $R_a = 10^2\,\Omega$ (referred to primary), and $b = 1$. These give

$$M' \sim 10 \quad \text{watt}^{-\frac{1}{2}}.$$

Take $Q_o = 10^4$, $\ell = 1$, $\beta = 2$ cm^{-1} and obtain

$$S_{max} \sim 1.5\times10^3 \text{ cm}.$$

---

* Due primarily to the isolation pad attenuator (see Fig. 14).

Finally, let $\Delta f = 20$ cps, $\alpha = 5$ dp, $P_a = 10^{-4}$ watts. Substituting these values in (99) gives

$$\gamma_{min} \sim 10^{-9} \text{ cm}^{-1}.$$

There are, of course, other sources of noise which raise in practice the value of the minimum detectable absorption coefficient:

(1) Low-frequency flicker noise from the first tube.

(2) Amplitude and frequency instability in the klystron oscillator and the modulation source.

(3) Corona noise from the high-voltage buses.

(4) Tube and microwave coaxial cable microphonism.

(5) "Gain-variation noise" from line voltage fluctuations.

The employment, however, of the differencing arrangement, the balanced lock-in amplifiers and low-pass filter as discussed in section G of part IV results in a considerable improvement in the signal-to-noise ratio. Experimentally, the spectrometer under the condition of zero Stark voltage was found to be capable of detecting absorption coefficients down to about 3×10^{-8} cm^{-1}.

VI. EXPERIMENTAL PROCEDURE

Contrary to the usual practice in spectroscopy, in the present experiment the resonant frequency ν_i' of absorption is varied while the frequency ν of the incident radiation is held fixed. By virtue of the symmetry of the line-shape factor (page 18) it is clear that this expression has the same form plotted against either of these frequencies.

Aside from the decided procedural convenience of operating at a fixed frequency for the incident radiation -- considering the selective nature of the resonant cavity, there is the feature that plotted against ν_i' the shape of an absorption line is simply the shape of the line-shape factor. With respect to ν as an abscissa, however, the shape of an absorption line is the line-shape factor weighted with the ν^2 factor in equation (29).

A. Basic Procedure.

By measuring the absorption coefficient of the gas for various values of the resonant frequency of a particular absorption line, a curve is obtained which has the form of the line-shape factor. Not only may the maximum absorption be determined therefrom, but also the frequency of peak of absorption and the line-breadth parameter $\Delta\nu$. Experimentally, the resonant frequency of a line is varied by varying the static electric field which creates the sublevels corresponding to the transition. The resonant frequency has been found already to be given by (equation 18)

$$\nu_i' \equiv \nu_{JKM}^{JKM-1} = \frac{\mu E}{h} \frac{K}{J(J+1)}.$$

For narrow-breadth lines (see page 22), then, as the static field is increased to a value E_0 such that

$$\nu_i' = \nu_0 ,$$

the cavity characteristic frequency to which the microwave signal source is set, the absorption coefficient will be very nearly maximum. This condition provides for computing the dipole moment from

$$\mu = \frac{h\nu_0}{E_0} \frac{J(J+1)}{K} , \tag{100}$$

for a particular rotational state J, K. Both ν_0 and E_0 can be measured to a high degree of precision.

In addition, a plot of the absorption coefficient versus the static field affords a means for calculating the line-breadth parameter for the state J, K; since

$$\Delta\nu = \frac{\mu \Delta E}{h} \frac{K}{J(J+1)} , \tag{101}$$

where ΔE is the half-width between half-intensity points. The effective collision cross section of the molecule can be computed now by means of equation (40).

A form of expression (29) which is particularly convenient for purposes of computation is the following:

$$\gamma = \frac{8\pi^2}{ckT} N\nu_0 |\mu_i''|^2 F(E, \Delta\nu) \frac{g_I e}{4} e^{-W_i''/kT} , \tag{102}$$

where

$$F(E, \Delta\nu) \equiv \frac{\frac{\Delta\nu}{\nu_0}}{\left[\frac{K}{J(J+1)} \frac{\mu E}{h\nu_0} - 1\right]^2 + \left[\frac{\Delta\nu}{\nu_0}\right]^2} + \frac{\frac{\Delta\nu}{\nu_0}}{\left[\frac{K}{J(J+1)} \frac{\mu E}{h\nu_0} + 1\right]^2 + \left[\frac{\Delta\nu}{\nu_0}\right]^2} .$$

Figure 18 is a plot of $F(E, \Delta\nu)$ for a typical narrow breadth line in terms of the dimensionless parameters $\mu E/h\nu_0$ and $\Delta\nu/\nu_0$.

B. Frequency-Sweep Technique.

Of considerable value in testing and adjusting the resonant cavity is a method whereby the cavity transmission characteristic is displayed on the monitoring cathode-ray oscilloscope. The saw-tooth sweep voltage from the oscilloscope is applied as modulation to the klystron reflector. In this way the microwave signal source is frequency modulated so that it sweeps repetitively through the cavity transmission curve.

For sufficiently high test-gas pressures the absorption line breadth will exceed the transmission curve width; and if the line is not too weak, the decrement in the Q of the curve displayed on the oscilloscope may be used to calculate the absorption coefficient by means of the relation derived in part V.

Since amplitude modulation necessarily attends the frequency modulation of the klystron output, a more precise technique is to survey pointwise the transmission curve with a monochromatic source, carefully adjusting the klystron output level to a fixed value for each reading.

If Q' and Q'_0 are the measured values of the quality factor with and without gas absorption, the absorption coefficient determined from equations (76) and (86) is

$$\gamma = \frac{\beta}{p}\left[\frac{Q'_0 - Q'}{Q'_0 Q'}\right]. \qquad (103)$$

C. Operating Techniques.

Preliminary to use of the spectrometer it is necessary to allow the high-vacuum system to run at least 24 hours to insure sufficient outgassing of the many surfaces of the cavity assembly. To minimize spark-breakdowns with application of the high voltage to the Stark electrodes, it is found advisable carefully to degrease the electrodes, the cavity cylinder, and the dielectric septum before assembly.

All electronic equipment is allowed at least one hour to reach thermal equilibrium in order to avoid excessive drifts.

1. Test gas injection.

After the Hyvac pump (Fig. 11) has evacuated the air from the injection-system plumbing, it is closed off. The outlet valve of the drier is also closed. A quantity of the test gas is passed into the drier, where it is allowed to stay in contact with the desiccant for several minutes. Next, the drier outlet valve is opened and the absorption cell is switched from the high vacuum to the gas-injection system. The drier outlet is closed and the system is evacuated again, the absorption cell being switched back to the high-vacuum system after the Hyvac pump has removed most of the gas. This flushing cycle is repeated once more; and, finally, the absorption cell is filled with the test gas plus a small quantity of sulphur hexafluoride, an additive whose purpose is to be described later.

2. Spectrometer adjustment.

The adjustment procedure starts with tuning the klystron, both mechanically and electronically, until it oscillates at the peak of

a mode curve and at the peak of the absorption-cavity transmission characteristic. About 10 db total pad is inserted between the source and the cavity to prevent excessive pulling (see Fig. 14). In addition, there is about 5 db of isolation pad between the cavity and the detection crystal. The variable-stub tuner is adjusted for a standing-wave ratio of less than 1.05 as indicated by the standing-wave detector.

Next, the variable attenuator in the balancing branch of the microwave bridge is adjusted to cancel most of the cavity signal as observed on the monitoring cathode-ray oscilloscope. With the bridge thus slightly unbalanced the phase-shift control (Figs. 14 and 15) is set for maximum response on the rough-adjustment meter following the balanced d-c amplifier.

The balancing branch is now adjusted for zero difference signal. The potentiometers in the plate circuits of the lock-in amplifiers and the balanced d-c amplifier provide for further adjustment until virtually a complete null obtains. The output of the d-c amplifier is finally switched from the meter to the Brush recorder amplifier.

3. Measurement procedure.

As the voltage from the high-voltage supply is slowly increased from zero, the static electric field across the Stark electrodes increases, as does the resonant frequency of the molecular absorption line. The unbalance of the microwave bridge resulting from the increased loss in the cavity absorption cell appears on the Brush recorder as a deflection proportional to the change in the absorption coefficient from the zero-field value.

The other channel of the recorder (Fig. 15) records on the same chart the voltage applied to one Stark electrode, from which the static field may be calculated as discussed above (page 38).

4. Sulphur hexafluoride additive and pressure limits.

Subjected to fields up to nearly 40,000 volts per cm the test gas readily fails if the pressure is too low. Of considerable value in increasing the effective spark-breakdown voltage is the fine thread chased on the inner surface of the dielectric septum as described on page 37.

In view of the desirability of dealing with narrow-breadth lines, pressures of at most an atmosphere, preferably lower, are to be sought. In practice, reduction of the gas pressure to an atmosphere and below results not only in sparkover as the static field is increased, but also in strong spurious corona noise which tends to mask the difference signal.

With the addition of a quantity (up to 20%) of sulphur hexafluoride (SF_6), it was found that the pressure might be safely lowered to somewhat less than a third of an atmosphere. Sulphur hexafluoride, a heavy non-polar molecule, composes a gas of high dielectric strength. It is used effectively as high-voltage gaseous insulation in Van de Graaff generators and elsewhere.(31) Further efforts to improve the dielectric strength in order that the pressure might be reduced even lower were futile. Various percentages of the test gas and the sulphur hexafluoride were tried; but a proportion of additive of more than 20% partial pressure of the total gained little in allowing a lower pressure, while seriously diluting the test gas.

The possibility of reducing the pressure way down to a value below the (pd) for minimum sparking voltage* was seriously considered. For pressures less than the order of a mm of Hg, unfortunately, field-inhomogeneity broadening will predominate and the absorption coefficient will decrease with further reduction in pressure (see III-B-4 and III-D-1).

---

* See J. Cobine, reference 23, page 164.

VII. EXPERIMENTAL RESULTS

Those substances which were studied in the course of developing the spectrometer and suitable experimental techniques included three symmetric-top molecules, NH_3, CH_3Cl, and SF_6; and two linear rotators, N_2O and CO_2.

The linear rotator, essentially a degenerate case of the symmetric-top for which the spin quantum number $K = 0$, can display no first-order Stark effect. The second-order effect observed for the slightly polar nitrous oxide is of little interest here.

A. Ammonia

1. Stark effect.

At the outset of the investigation, the most promising symmetric-top molecule appeared to be NH_3. A list of important molecular parameters appears in Table 2. An easily handled, readily procured gas, ammonia has a fairly large dipole moment, $\mu = 1.45$ Debyes, which is desirable to keep the resonant static field E_0 low. From equation (97) we calculate $E_0 = 24.0$ kv/cm for the $J = K = 1$ lines and $\nu_0 = 8.77$ kmc and a Stark voltage of 42.8 kv for resonance. The NH_3 molecule has, furthermore, a large non-unique reciprocal moment of inertia, $B_0 = 298$ kmc. As is evident from examination of equations (35) and (29), a large B_0 means a low partition function and hence a strong, easily detected absorption line. In addition, a large B_0 means a negligible second-order correction (equation 16) to the perturbation energy, since

$$\frac{\mu E_0}{h} \sim \nu_0 << B_0 .$$

Early calculations, which were most encouraging, on the absorption coefficient for the $J = K = 1$ lines of NH_3 were made essentially as follows:

At a pressure of 1 atmosphere the gas should withstand an electric field of the order of 24 kv/cm for an electrode gap of approximately 2 cm since ammonia has about the same dielectric strength as air.* Assuming a kinetic-theory collision cross section of 40 $\mathring{A}^2$ for the NH_3 molecule, one calculates a line-breadth parameter of $\Delta\nu = 1.4$ kmc at $T = T_0 \equiv 300^\circ K$ by means of expression (40). This indicates narrow-breadth lines of the form of Figure 18, a desirable condition as emphasized previously.

The hydrogen nuclei each have a spin $\frac{1}{2}$; so, assuming the molecules to be mostly in the ground vibrational state ($\nu = 0$), one finds the statistical weight and the rotational partition function to be $g_I = 2$ and $Z = 571$ from equations (32) and (35) for $A_0 = 189$ kmc. The average energy of the two levels involved in the transition is approximately that of the $J = K = 1$ level; that is, $\bar{W}_I^j = \frac{1}{2}(W_{11M} W_{11M-1}) \approx W_{11} = h$ (784 kmc). Now kT_0/h 6000 kmc (see Fig. 1), consequently $\exp(-\bar{W}_I^j/kT_0)$ is roughly unity.

Substitution, then, of the foregoing values and $N = 2.7 \times 10^{19} cm^{-3}$ in (43) gives

$$\gamma_0 \approx 2 \times 10^{-4} cm^{-1}$$

---

* Cobine, reference 23, page 166.

for the maximum absorption coefficient -- an easily detectable value. This corresponds to an unloaded cavity Q of about 5000 from (76) for $Q_0 \sim 10^4$ and $P \sim 1$. If the sweep-frequency technique is used, the quality factors as measured from the oscilloscope displays would be about 1/3 of these values for optimum coupling.

Most interesting of all, however, is the fact that the pure rotational lines of ammonia lie in the infrared and are therefore inaccessible to the usual microwave techniques. Equation (9) gives for the lowest rotational line $\nu''_{01} = 2B_0 = 596$ kmc, which is well above the microwave spectrum.

By the experimental procedure which is the topic of this thesis, it might be possible to split the relatively high $J = K = 1$ level into sublevels differing by the considerably lower energy of the microwave quantum.

These hopes were not wholly realized; under test the ammonia gas displayed a monotonic rise in absorption as the static field was increased. Figure 19 shows the results for two values of pressure. Note that the zero-field absorption does not appear. No maximum in absorption could be found, even at the lowest pressure attainable. The reasons for this behavior are to be discussed later.

2. Inversion lines.

In the course of the investigation with ammonia, it was noted that the cavity transmission curve appearing on the monitoring oscilloscope was appreciably broadened when the gas was injected into the absorption cell, even in the absence of the static field. At first,

the cause of this effect was not understood. Eventually it became clear that the excessive absorption was due to the microwave inversion lines* of ammonia sufficiently collision broadened so that their wings add to appreciable absorption at the cavity frequency. Figure 20 shows a plot of the absorption coefficient versus pressure as determined by means of equation (102) from experimental data. The quality factors were computed by dividing the frequency of peak transmission by the frequency difference between the half-peak transmission points at various pressures.

The absorption-cell space factor (page 44) is readily determined, if it is assumed that, as a first approximation, the microwave electric field distribution in the cavity is unaltered by the presence of the dielectric septum:

$$p \equiv \frac{\int_{cell} u\,dV}{\int_{cell} u\,dV} = \frac{\int_0^{b_1} \rho J_1^2(\xi_1 \frac{\rho}{a})\,d\rho}{\int_0^{a} \rho J_1^2(\xi_1 \frac{\rho}{a})\,d\rho} \qquad (104)$$

for the fields given by (66). Equation (104) yields

$$p = .75 \frac{[J_1^2(\xi_1.75) + J_0^2(\xi_1.75)]\xi_1.75 - 2J_1(\xi_1.75)J_0(\xi_1.75)}{\xi_1 J_0^2(\xi_1)} . \qquad (105)$$

For the dimensions listed in Table 1, the space factor is computed to be

$$p = 85.9\% .$$

---

* The strongest line is centered at 23.9 kmc.

Cleeton and Williams[1] have made measurements of inversion absorption at atmospheric pressure. Their value for the absorption coefficient is indicated in Figure 20 for comparison. Remarkably good agreement is evident, so there is little doubt that energy was being lost in the process of inversion doubling.

B. Methyl Chloride.

The next symmetric-top molecule to be investigated was methyl chloride (CH_3Cl), a molecule which displays no inversion lines in the microwave region. The CH_3Cl molecule has, however, a relatively low non-unique reciprocal moment of inertia $B_0 = 13.3$ kmc (see Table 2); which means weaker lines than for NH_3, as well as an appreciable second-order correction to the perturbation energy.* Fortunately CH_3Cl has a higher dipole moment, $\mu = 1.86$ Debyes, than does NH_3, and consequently a lower Stark voltage for resonance. Since the absorption coefficient depends on the square of the dipole moment as is explicit in equation (29), the high μ tends to compensate for the lower B_0.

It was during the tests on methyl chloride that the practice of adding sulphur hexafluoride was initiated. By this means the minimum sparkover pressure was reduced from a value of about $1\frac{1}{2}$ atmospheres to a value of less than 1/3 atmosphere.

Figure 21 is a plot of the increase in the absorption coefficient from its zero-field value with respect to the Stark voltage. The values shown are an average for several runs recorded on the Brush recorder.

---

* The correction calculated by (16) for $J = K = 1$ is about 3.5% at resonance.

These data were computed by means of equation (89) and (90) for the following values: ν_o = 9.353 kmc; ρ = 0.859; Q_o' = 3.1×10^3. Again it is noted that no maximum in absorption is observed, even at the relatively low pressure of 21.3 cm of Hg.

C. Carbon Dioxide and Sulphur Hexafluoride.

As a control experiment two non-polar gases, CO_2 and SF_6 were tested. Neither of these gases displayed increasing absorption with increase of the Stark voltage as did NH_3 and CH_3Cl. Indeed, a slight negative difference signal was observed. This virtual increase in cavity transmission probably arises from increase in corona noise with increasing voltage, a signal which effectively augments the microwave signal.

VIII. DISCUSSION

A. Ammonia Inversion Absorption.

As has been explained theoretically by D. M. Dennison and others[34], the NH_3 molecule can, in terms of a pyramidal model, turn itself inside out by the phenomenon of the nitrogen passing axially through the plane defined by the three hydrogen atoms. Quantum mechanically, this means that the nitrogen resides in two equal potential wells separated by a barrier 2076 cm^{-1} high through which the nitrogen atom tunnels by quantum-mechanical resonance. The average time for the excursion is about 2.5×10^{-11} sec. An X-band microwave having a period of the order of 10^{-10} sec. finds, then a zero-average dipole moment. Therefore, no first-order Stark effect of pure rotational levels is to be expected from NH_3 at frequencies near the inversion spectrum, because there is an equal probability of finding the N atom on either side of the H_3 plane.

Under the perturbation of a strong static field, the potential distribution becomes asymmetrical and a second-order Stark effect appears. The results shown in Figure 19 are doubtless due to second-order perturbations. This difficulty with the inversion phenomenon was not appreciated at the outset of the investigation.

B. Collision Cross Section of Methyl Chloride.

The CH_3Cl molecule should display a first-order Stark effect since it has no microwave inversion spectrum. Experimentally, however, no resonance is found.

The explanation of this behavior most probably lies in the high effective collision cross section of the molecule, which gives rise to excessive collision broadening of the absorption lines. Virtually no information is available on the effective collision cross section of CH_3Cl. Coles* assumes a value of 1000 $\mathring{A}^2$, which exceeds the kinetic-theory collision cross section approximately 25 fold! From equation (40) one finds a line-breadth parameter $\Delta\nu = 27.1$ mc per mm of Hg pressure. At the lowest experimentally attainable pressure p = 21.3 cm, $\Delta\nu = 5.78$ kmc, a value which is decidedly comparable to the resonant frequency 9.353 kmc.

To support the foregoing contention, it is interesting to plot the first few absorption lines as predicted by formula (102). Figure 22 gives the factor

$$\sum_{M=-J}^{M=+J} g_I \exp\left(-\bar{W}^{JKM-1}_{JKM}/kT_0\right)\left(\mu^{JKM-1}_{JKM}/\mu\right)^2 F(\epsilon,\Delta\nu)$$

for the J = K = 1, 2, 3, 4, 5 lines over the range of experimental investigation. While lines above J = K = 5 contribute to the zero field absorption, they have little effect apparently on the slope of the total absorption curve. Evidently, the peak of J = K = 1 line, which is of particular interest, is lost in the wings of neighboring lines.

The sum of the first five lines multiplied by the factor $(8\pi^2/ck) \times (N\nu/\mu^2/T)$ is plotted in Figure 21 for comparison with the experimental results. The zero-field value is subtracted off since it is not significant here.

---

* Reference 2, page 51.

Again it is assumed that most of the molecules are in the ground vibrational state at room temperature. The vibrational partition function (34), furthermore, is nearly unity since the lowest fundamental frequency $\bar{\nu}_3 = 732$ cm^{-1} or about 22 F, a value well above kT_0/h (see Fig. 1).

As has been discussed by several authors* the high effective collision cross section of polar molecules such as CH_3Cl very likely results from dipole-dipole interactions. The collision cross section determined from kinetic theory is evidently much too small to account for the observed broadening of rotational lines. Much work yet remains to be done on this problem, both by theory and by experiment.

C. Paramagnetic Resonance Absorption Analogy.

It is interesting to note the similarity between the present experiment and the recent experiments(36,37) on microwave resonance absorption in paramagnetic salts and on nuclear magnetic resonance at radio frequencies. These experiments are conducted by placing a substance between the poles of an electromagnet, the field of which removes the $(2J + 1)$-fold degeneracy of the energy levels. The resulting split levels are populated according to a Boltzmann distribution and have energy differences between adjacent levels given approximately by

$$\Delta W = g \mu_m B \,, \tag{106}$$

where g is the gyromagnetic ratio, μ_m is the Bohr or nuclear magneton, and B is the static magnetic field.

---

* Cf. Anderson, reference 35 for a theoretical treatment.

When a magnetic field of frequency ν' normal to the static field is applied, the transition probability and hence the power absorption from the incident radiation reaches a maximum as the static field is varied. The extreme occurs when

$$h\nu' = g\mu_m B . \tag{107}$$

This expression is quite similar in structure to (18) which gives

$$h\nu' = \frac{K}{J(J+1)}\mu E .$$

It was indeed, consideration of the possibilities of conducting an analogous "microwave paraelectric resonance absorption experiment" which led the writer to the present investigation.

D. Experimental Accuracy.

In this exploratory research no great care was taken in the interest of precision. Until some means is devised for extending the measurements to the region of narrow-breadth lines, it is clear that this position is justified.

IX. CONCLUSIONS

A. Present Experiment.

While in the absence of experimental evidence indicating distinct spectral lines, one is hesitant to conclude that direct transitions between rotational sublevels were observed. The surprisingly good agreement between theory and experiment found for methyl chloride is, nevertheless, most significant -- if not conclusive. The failure, moreover, of the non-polar molecules tested to display such marked and reproducible dependence of absorption on Stark voltage under the same experimental conditions lends considerable strength to the contention that the observed absorption for ammonia and methyl chloride results from pure rotational transitions.

The spectrometer as it was designed and built proved to be adequate, for the most part, to the task undertaken. No doubt further refinement is necessary if the absorption lines are to be resolved. It is clear that some means must be devised which will permit a reduction of the order of 10 fold or more in test-gas pressure to reach the region of narrow-breadth lines.

B. Suggestion for Further Research.

1. Polar gases.

First, with respect to the problem of pressure reduction there are several possible solutions:

a. Retain the resonant cavity design but reduce the frequency and hence the static electric field. To provide for the attendant decrease in the absorption coefficient the ultimate sensitivity of the spectrometer will have to be increased.

b. Retain the resonant cavity design in the X-band and simultaneously micro-pulse the Stark field and the klystron oscillator. Two hydrogen thyratrons, one for the positive, the other for the negative lead, might be employed to switch the output of the high-voltage doubler described above. It might be possible to reduce considerably the gas pressure and still secure sufficient dielectric strength for the short interval during which the high field is impressed.

2. Liquids and solids.

Molecular rotation in liquids and solids is inhibited by strong interaction forces.(38) In the microwave region, however, many liquids display absorption peaks and associated anomalous dispersion. It would be most interesting to try to measure direct transitions between sublevels of dilute solutions of polar molecules in non-polar solvents. No doubt the absorption lines would be very broad, but the problem of dielectric strength would be considerably relieved.

One might determine in this way the relaxation time of the molecular dipole, as well as the loss factor which appears in the Debye theory(4) as a function of Stark voltage.

3. Molecular modulation.

Another technique which may be worthy of investigation is that whereby the Stark voltage is partially modulated with a sine wave. The cavity output signal would be, for low modulation levels, nearly proportional to the slope of the absorption line. Much more amplification in the detection system is, of course, required.

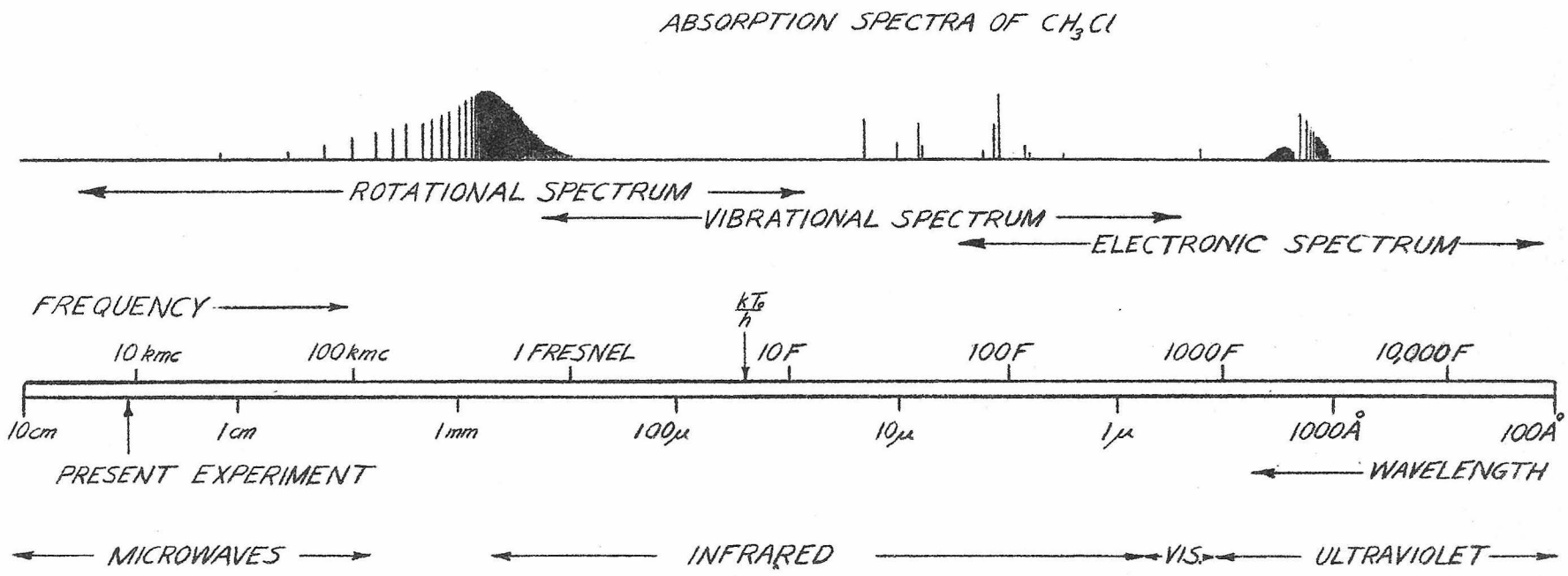

Figure 1. SPECTRAL POSITION OF MICROWAVES

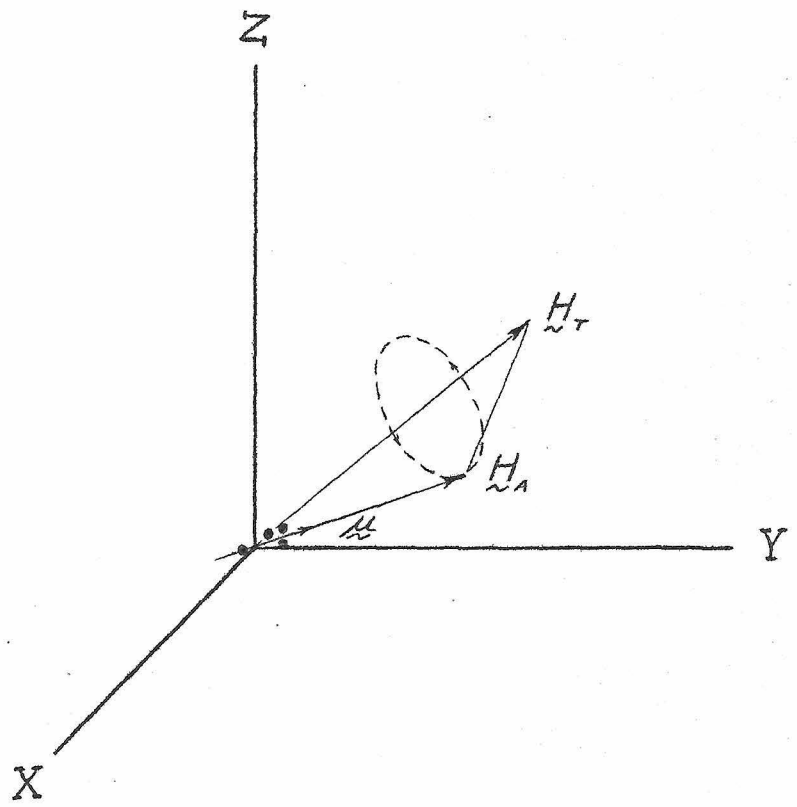

Figure 2. RIGID SYMMETRIC-TOP MOLECULE

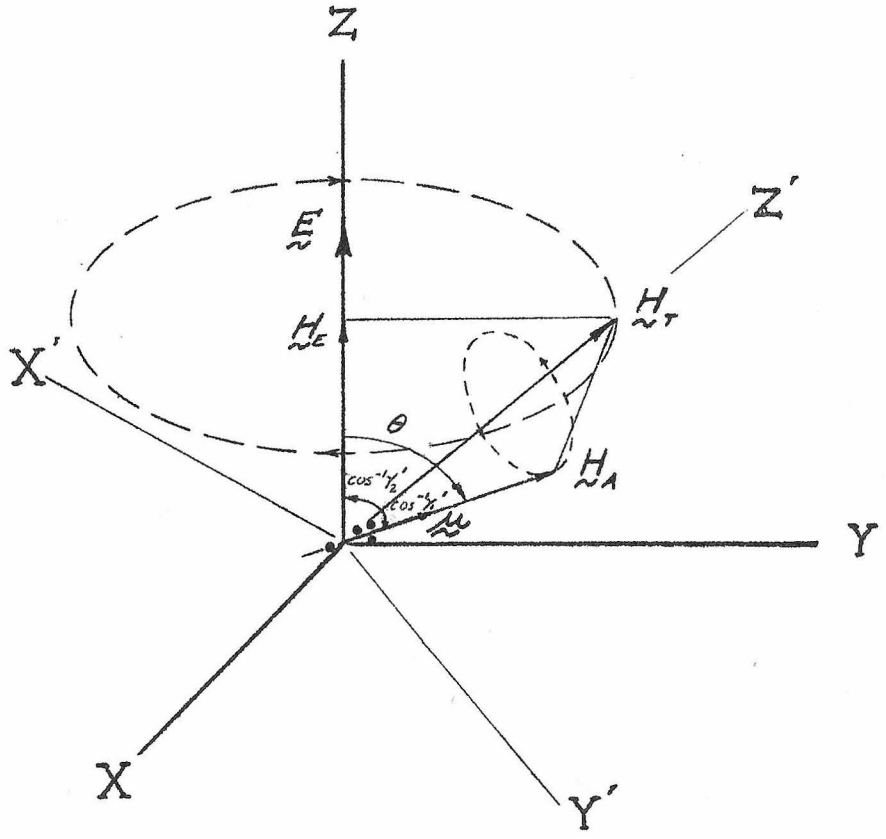

Figure 3. RIGID SYMMETRIC-TOP MOLECULE IN STATIC ELECTRIC FIELD

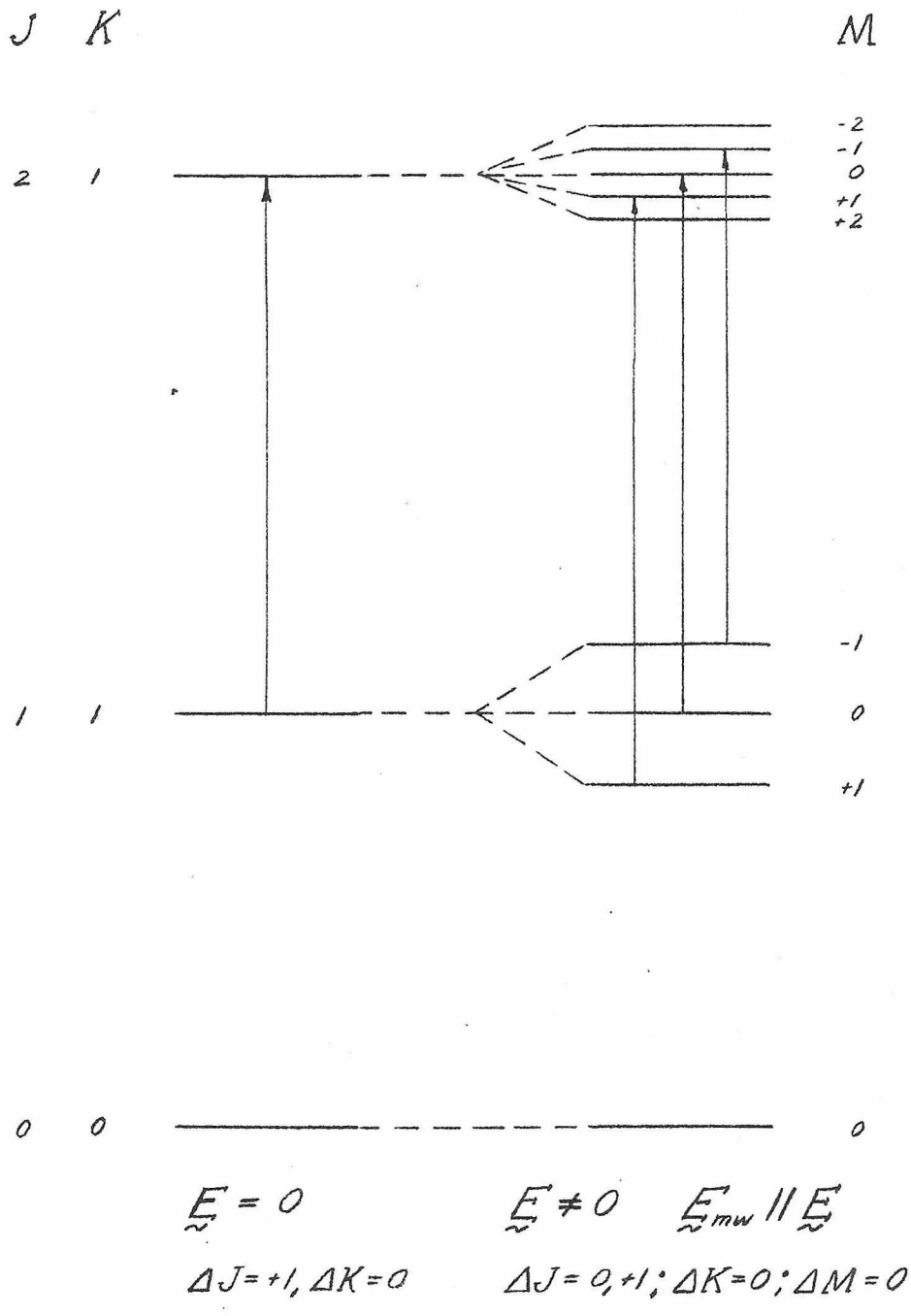

Figure 4. FIRST-ORDER STARK SPLITTING: MICROWAVE ELECTRIC VECTOR PARALIEL TO STATIC FIELD

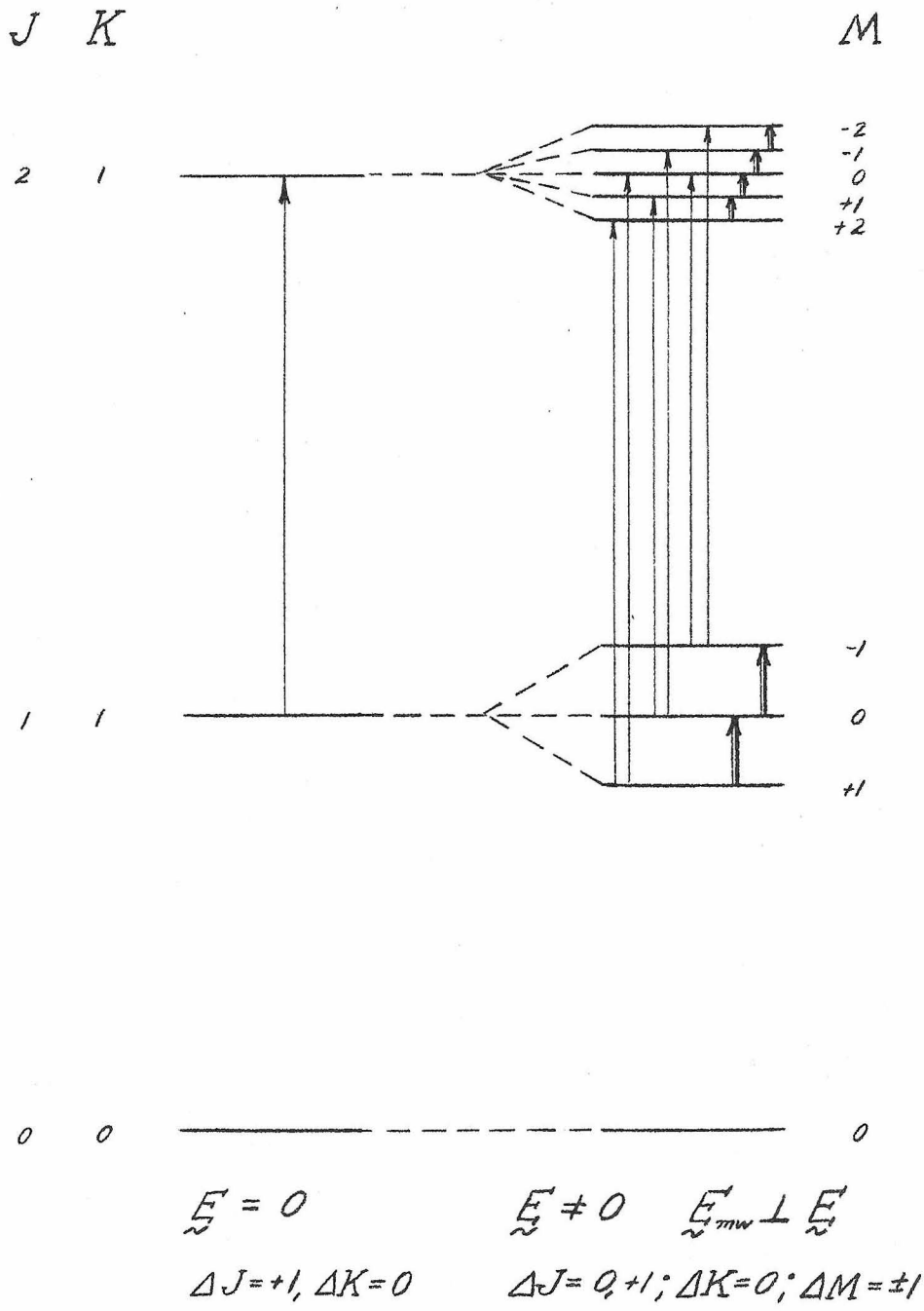

Figure 5. FIRST-ORDER STARK SPLITTING: MICROWAVE ELECTRIC VECTOR PERPENDICULAR TO STATIC FIELD

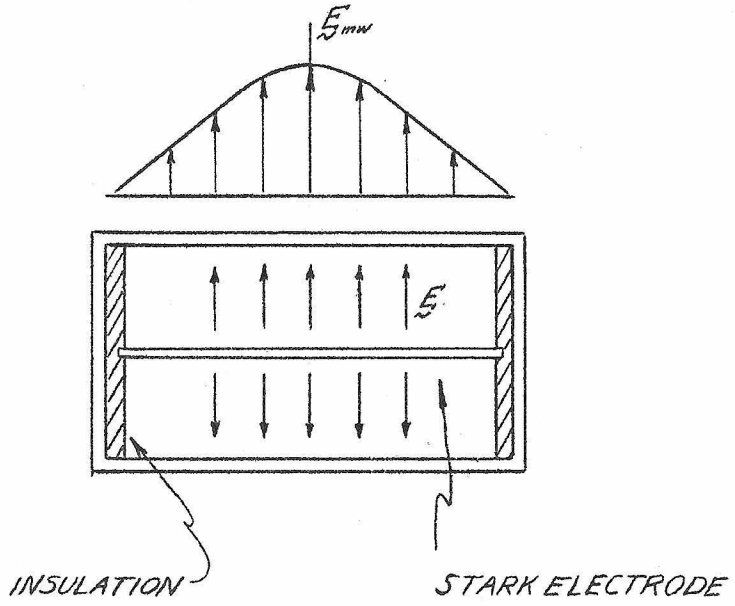

Figure 6. WAVE-GUIDE ABSORPTION CELL FOR STARK SPLITTING: $E_{mw} \| E$

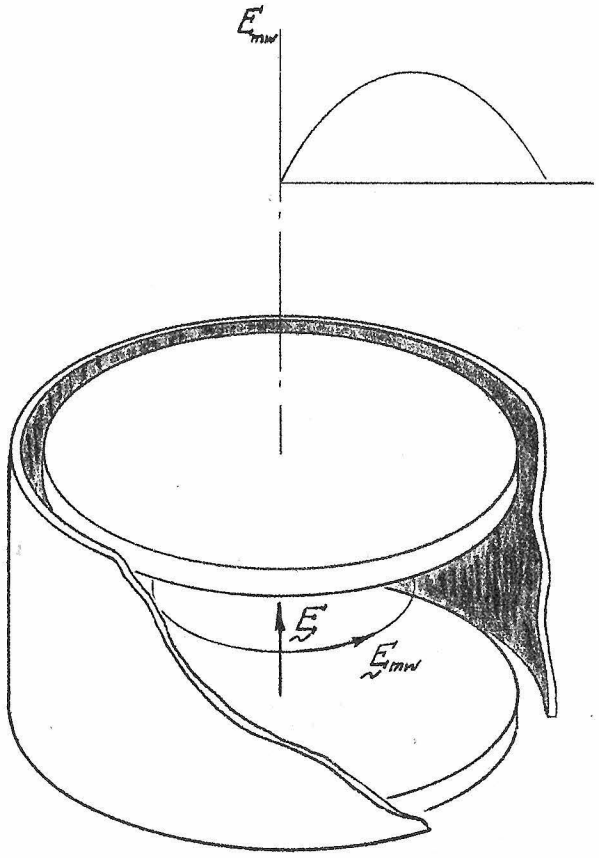

Figure 7. RESONANT-CAVITY ABSORPTION CELL FOR STARK SPLITTING: $\tilde{E}_{mw} \perp \tilde{E}$, TE_{01p} MODES

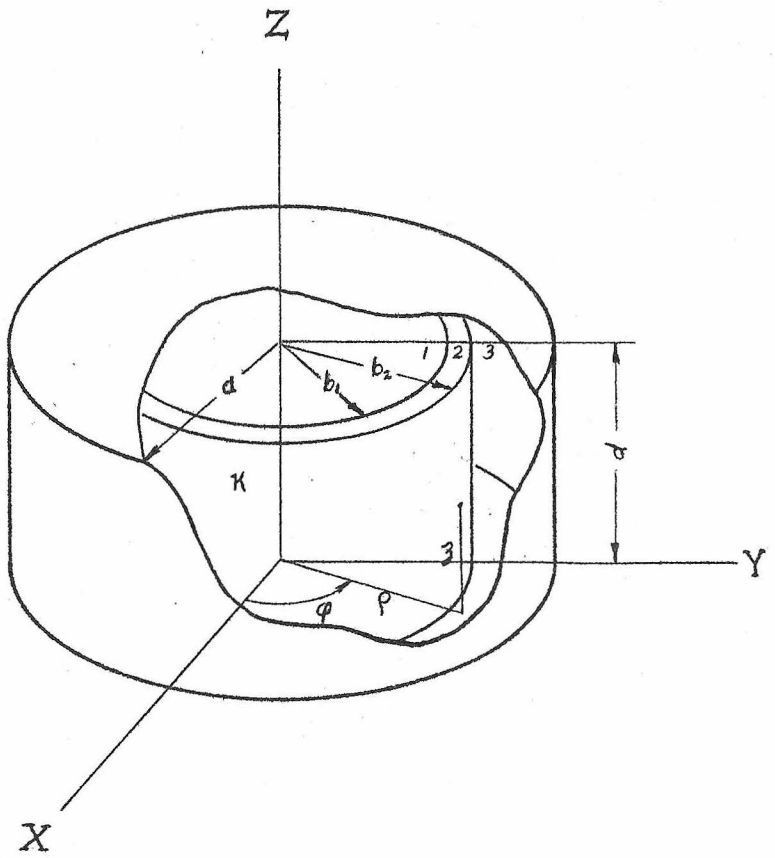

Figure 8. DIELECTRIC SEPTUM
FOR CONFINING GAS

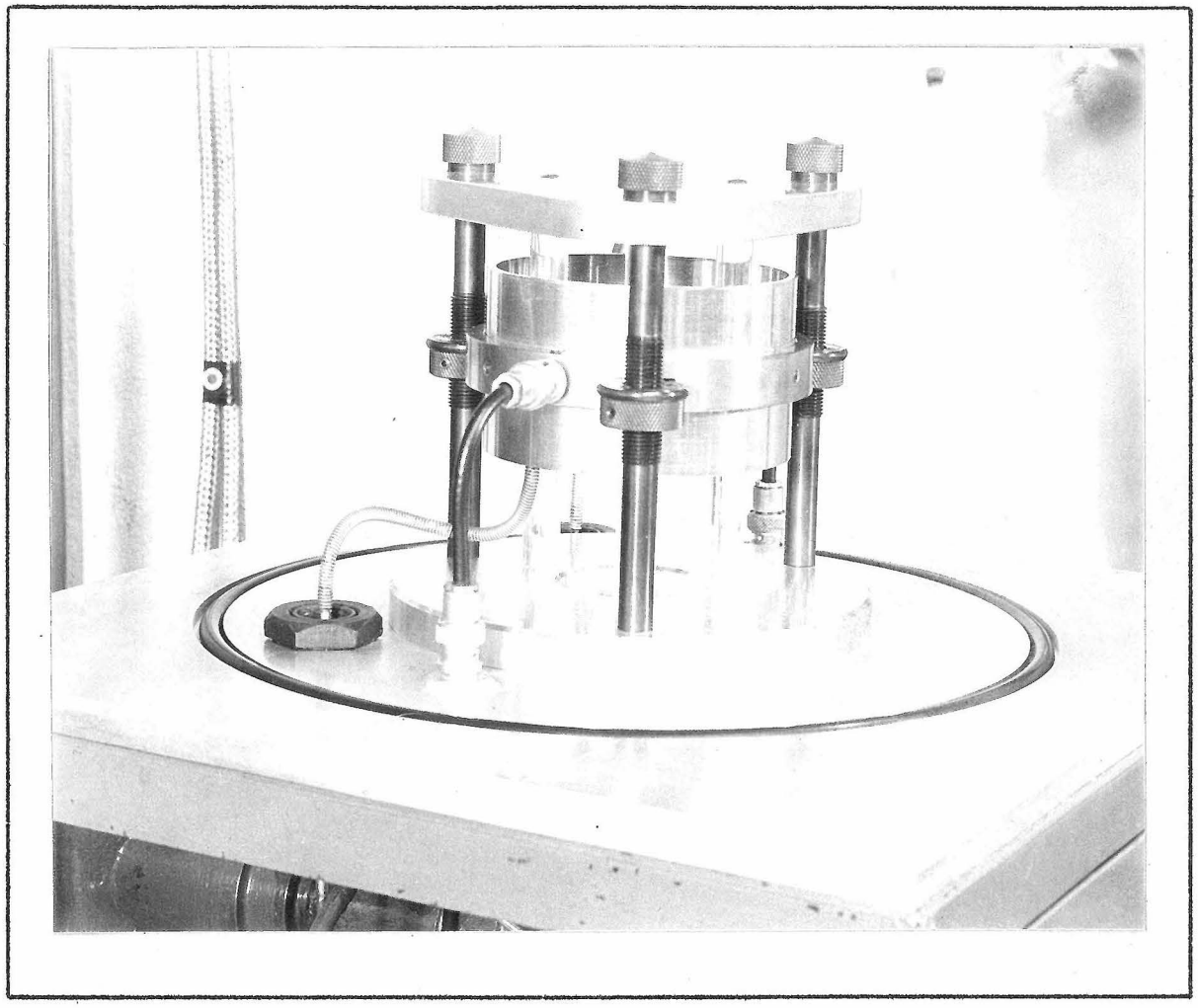

Figure 9. RESONANT-CAVITY ASSEMBLY

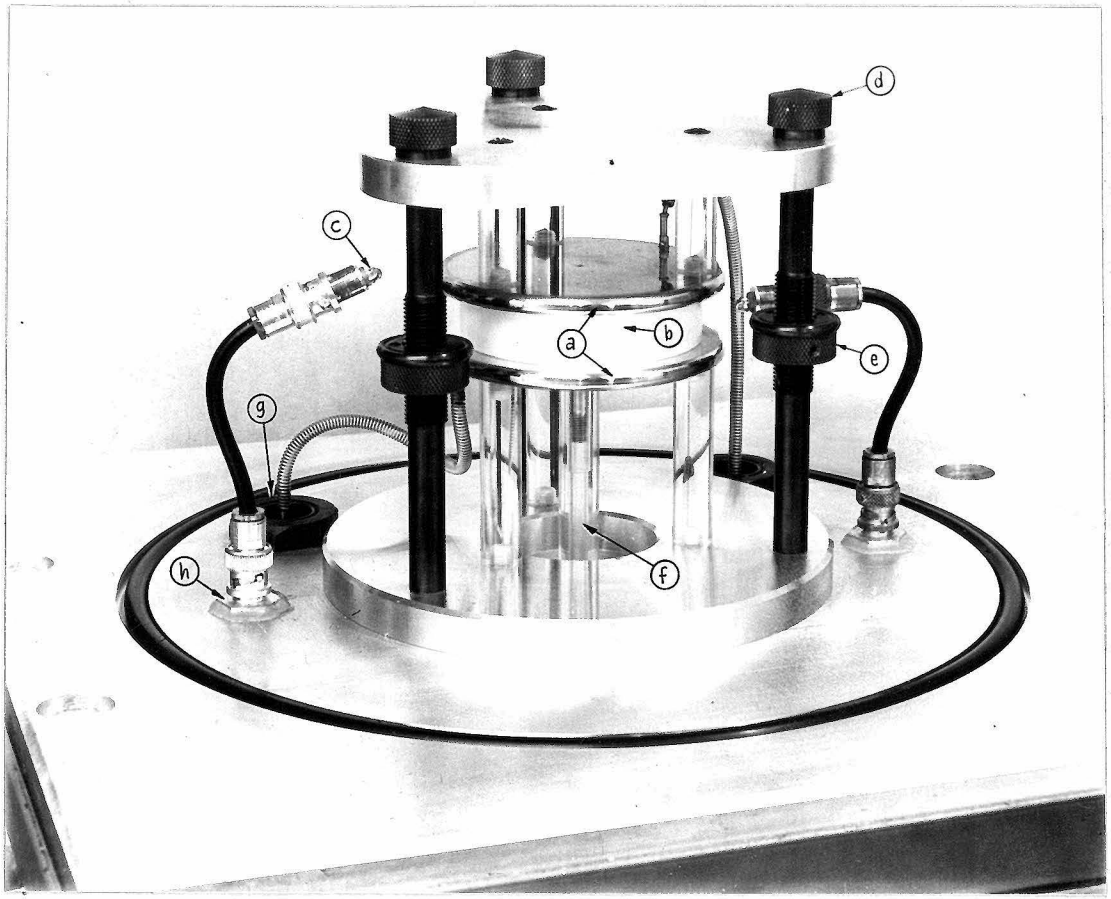

Figure 10. ABSORPTION-CELL ASSEMBLY

(a) Stark Electrodes

(b) Dielectric Septum

(c) Coupling Loop

(d) Electrode Adjustment

(e) Cylinder Adjustment

(f) Gas Injection Duct

(g) High Voltage Vacuum Bushing

(h) Microwave Vacuum Bushing

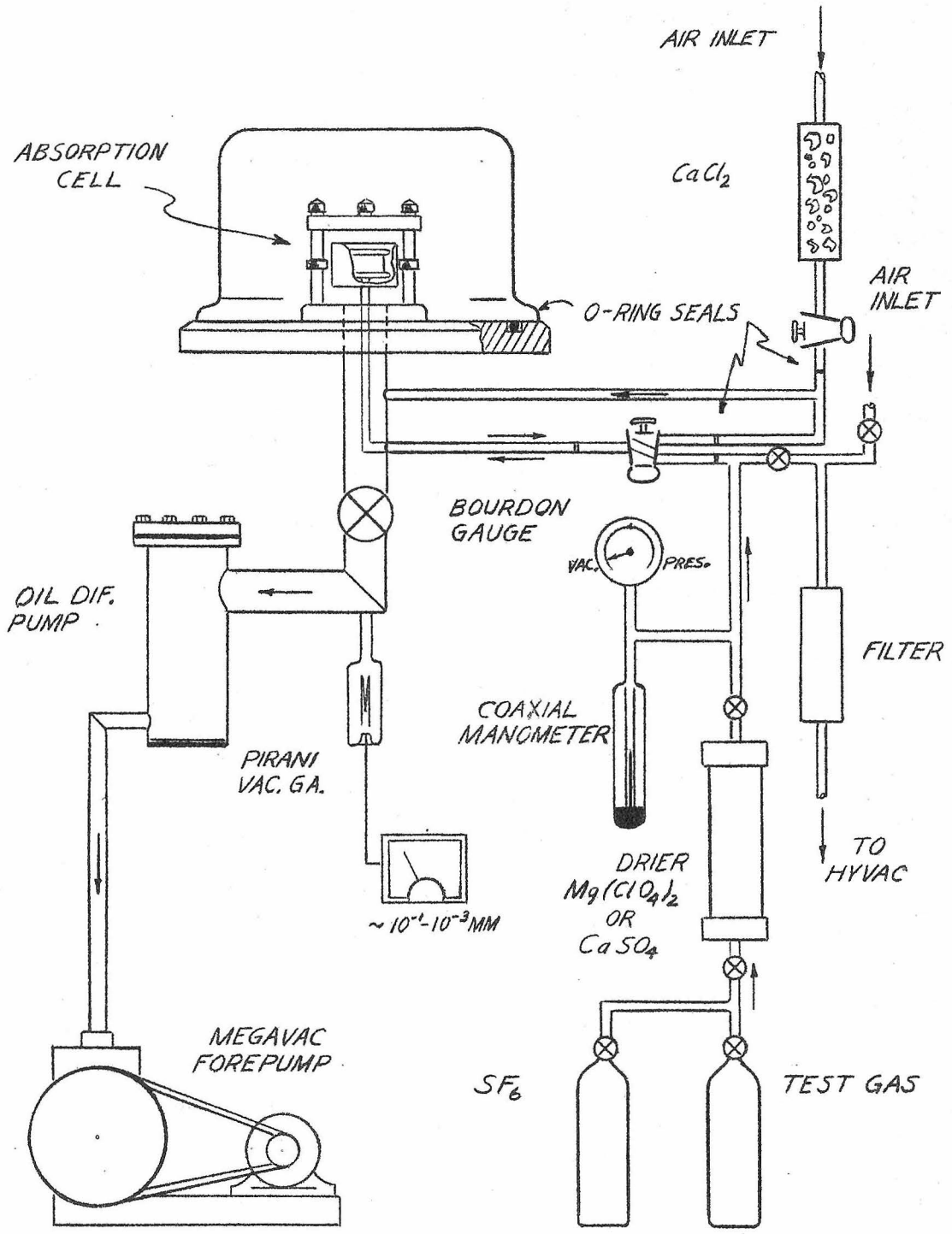

Figure 11. HIGH-VACUUM SYSTEM AND GAS-INJECTION SYSTEM

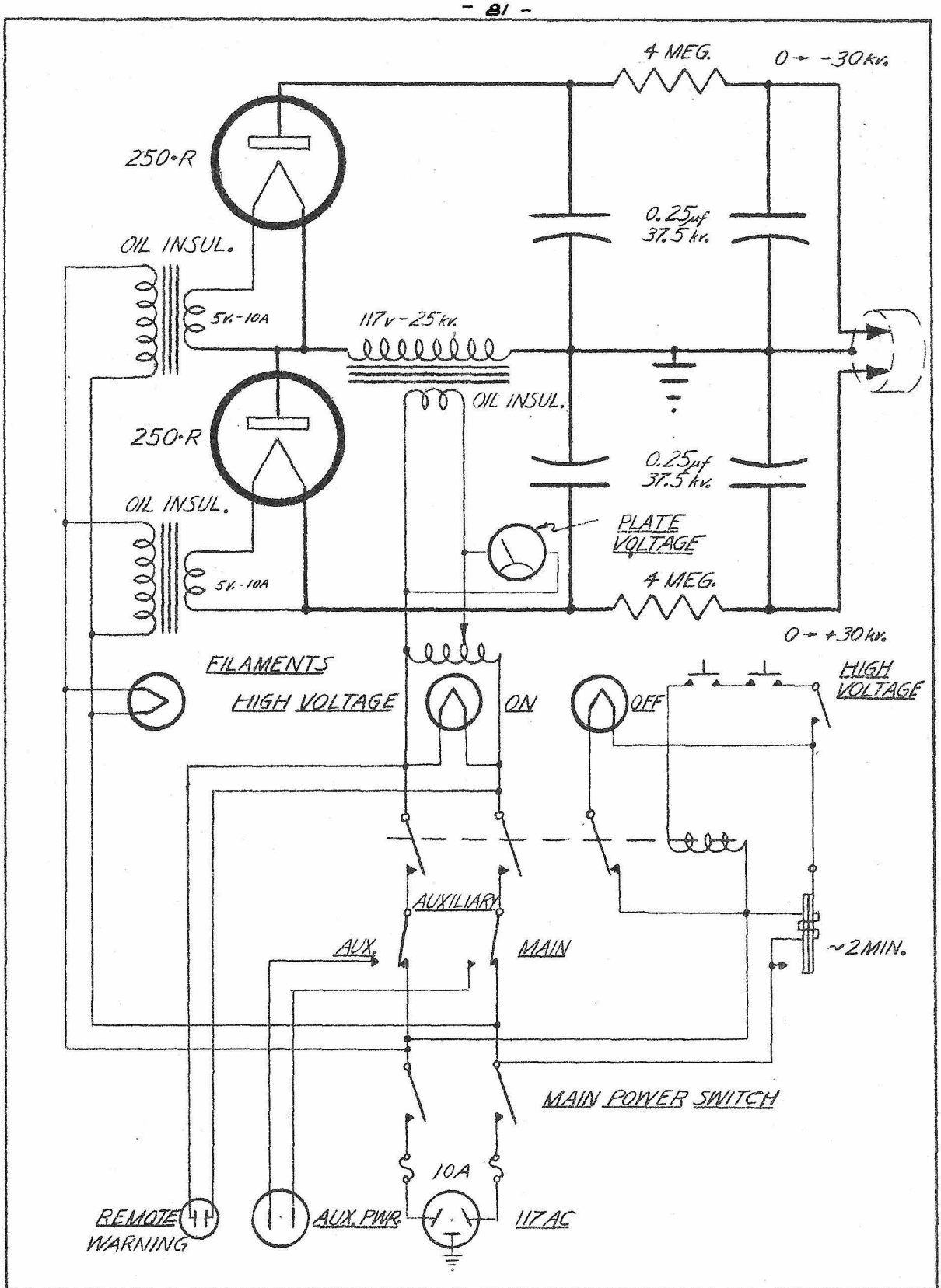

Figure 12. HIGH-VOLTAGE SUPPLY: SCHEMATIC DIAGRAM

FRONT VIEW

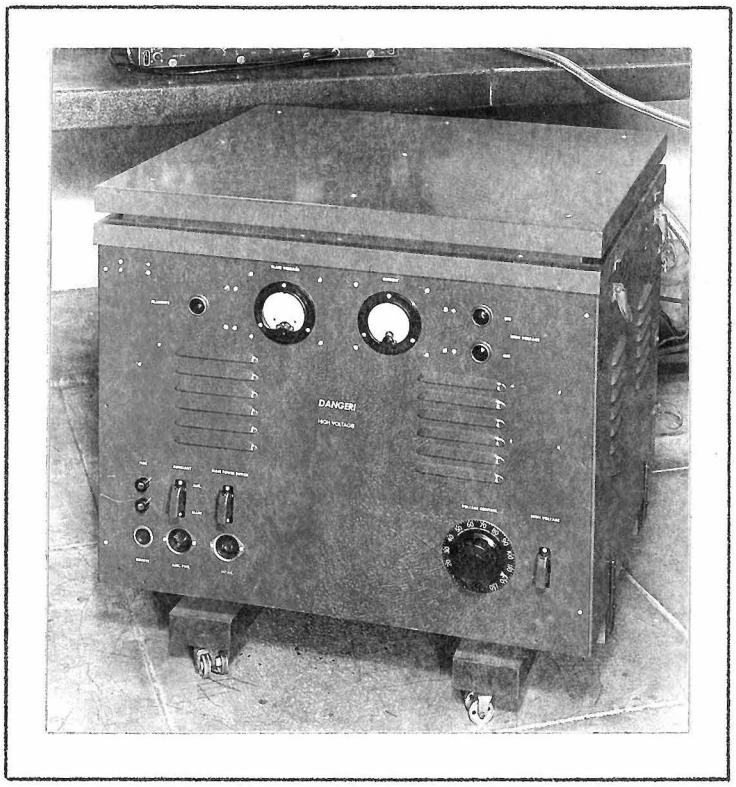

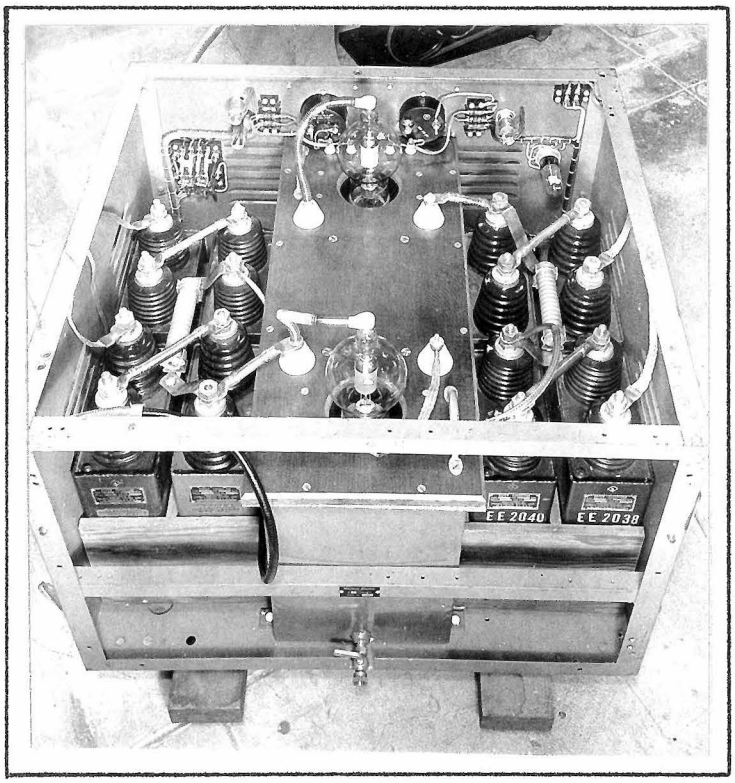

REAR VIEW

Figure 13. HIGH-VOLTAGE SUPPLY

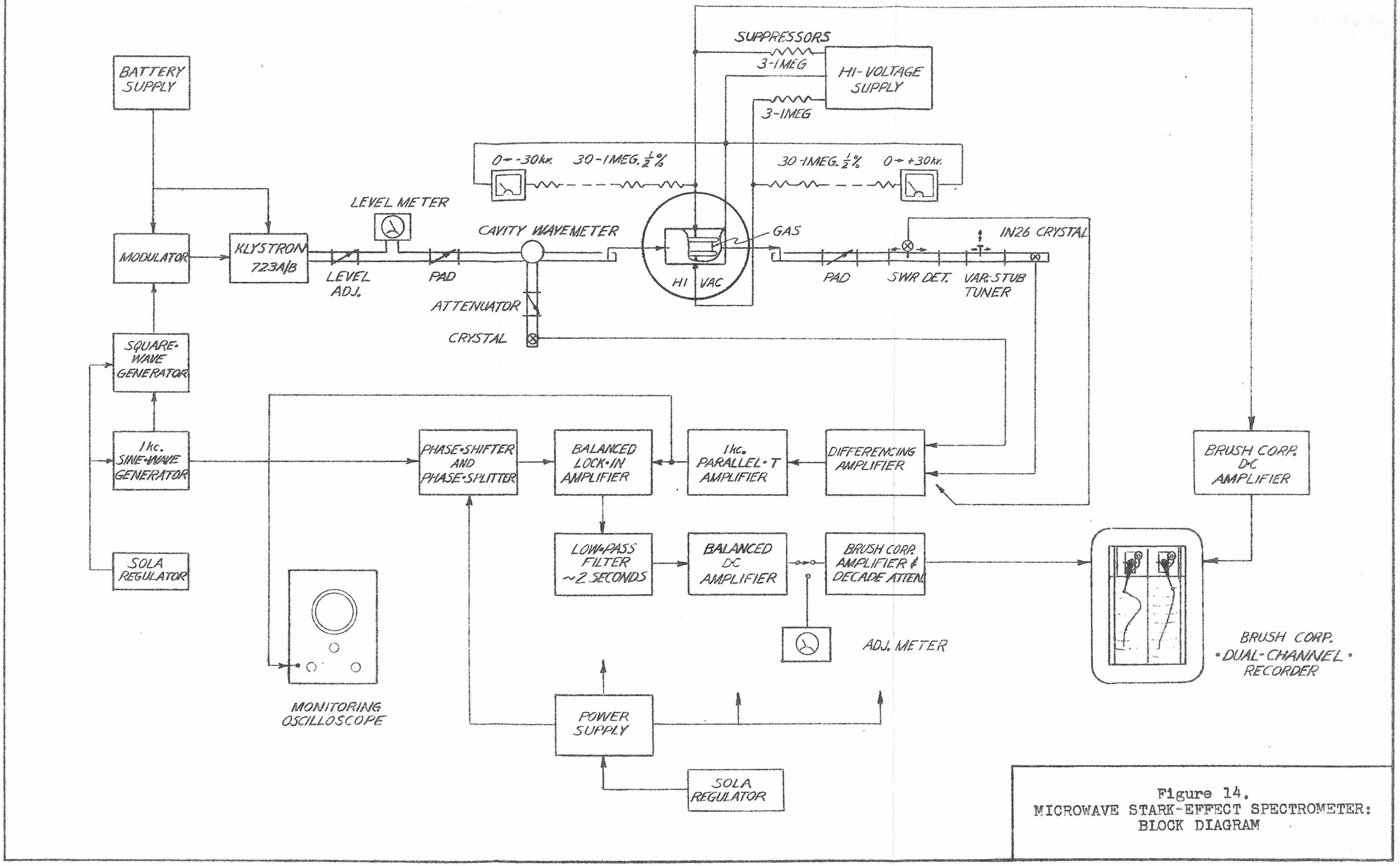

Figure 14.
MICROWAVE STARK-EFFECT SPECTROMETER:
BLOCK DIAGRAM

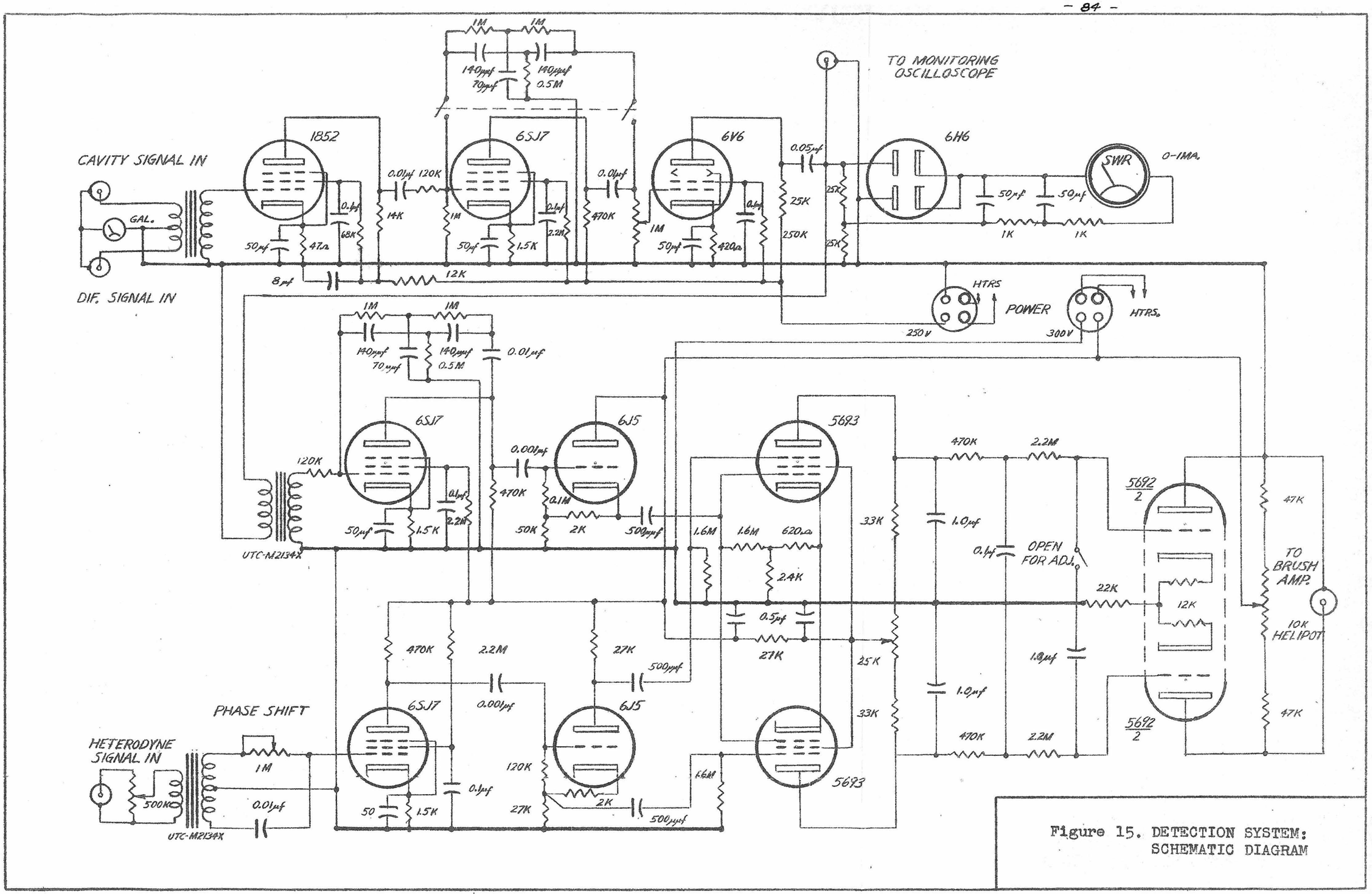

Figure 15. DETECTION SYSTEM: SCHEMATIC DIAGRAM

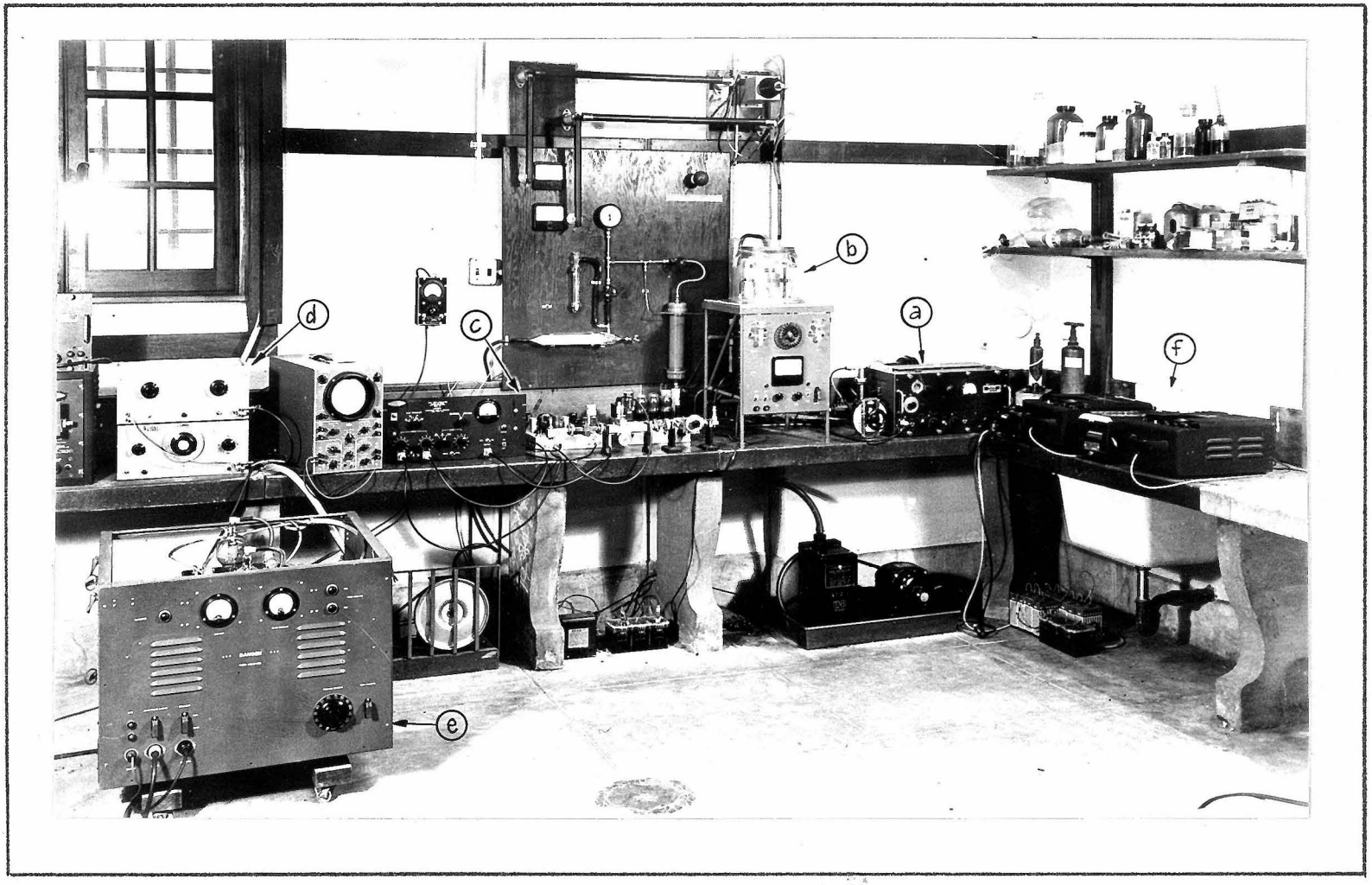

Figure 16. MICROWAVE STARK-EFFECT SPECTROMETER

(a) Microwave Source
(b) Absorption Cell
(c) Detection System
(d) Modulation Source
(e) High-Voltage Supply
(f) Brush Recorder

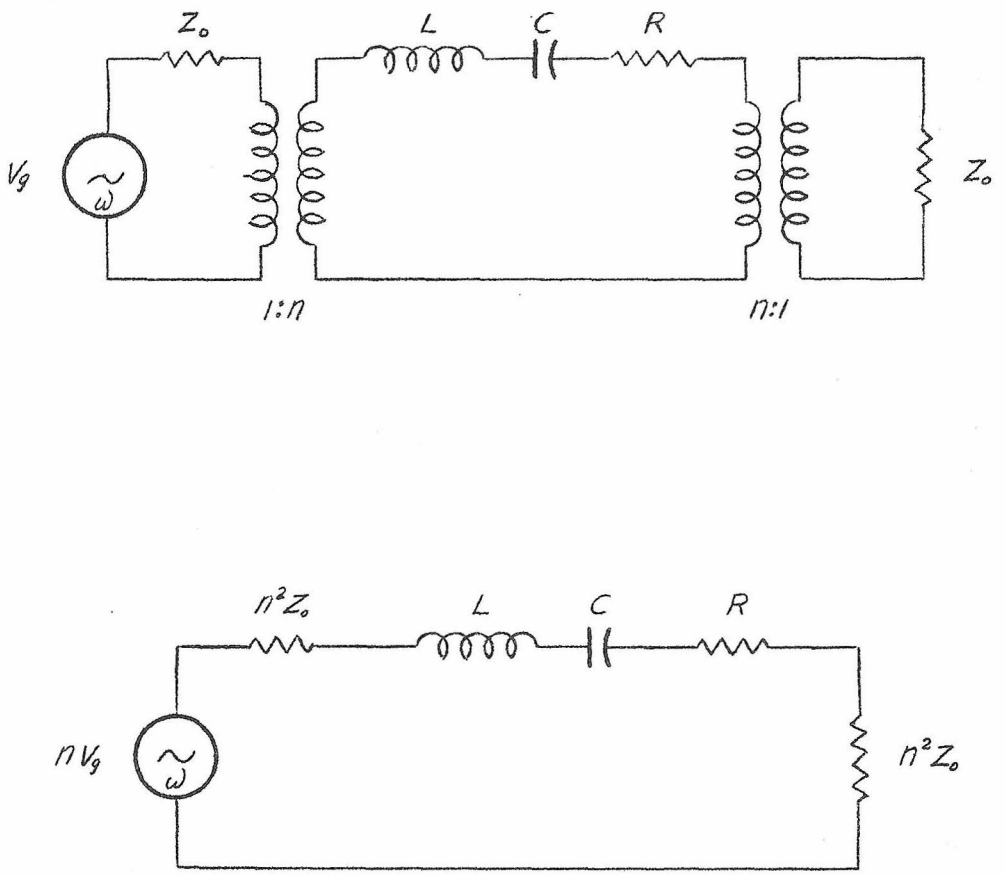

Figure 17. RESONANT-CAVITY EQUIVALENT TRANSMISSION CIRCUIT

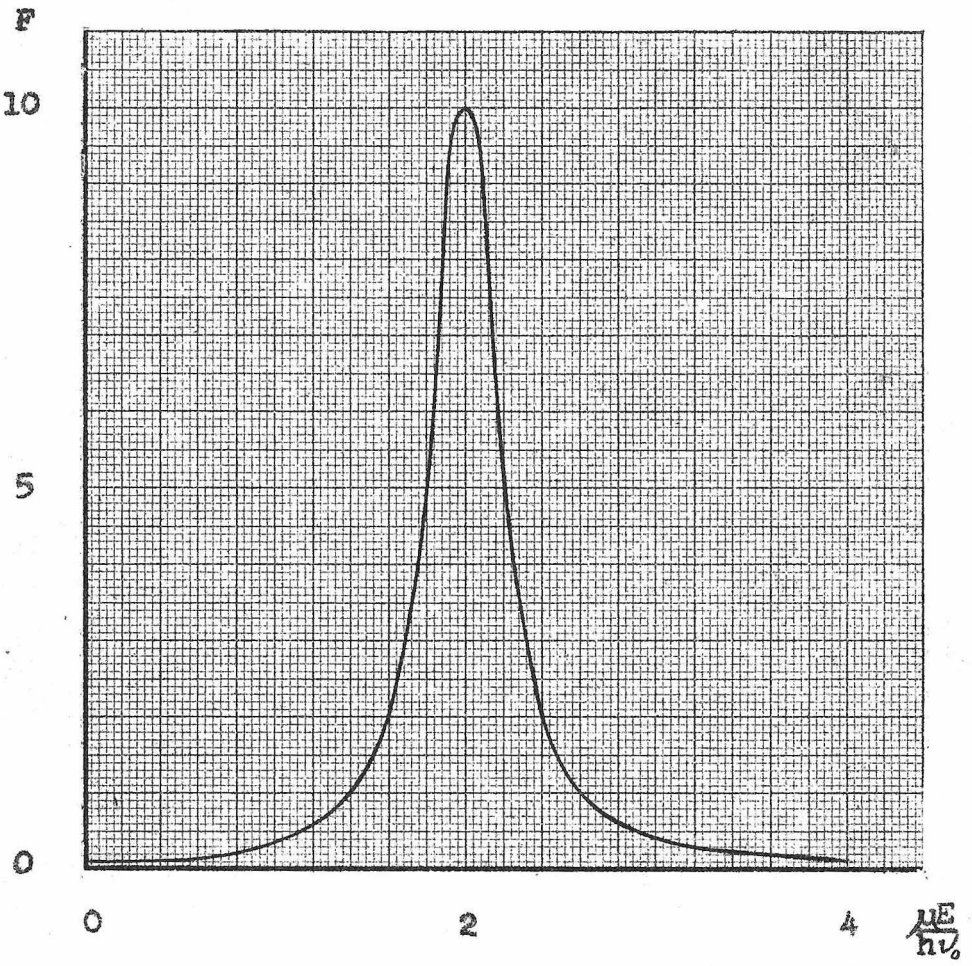

Figure 18. NARROW-BREADTH ABSORPTION LINE

$J = K = 1 \qquad \frac{\Delta\nu}{\nu_0} = 0.1$

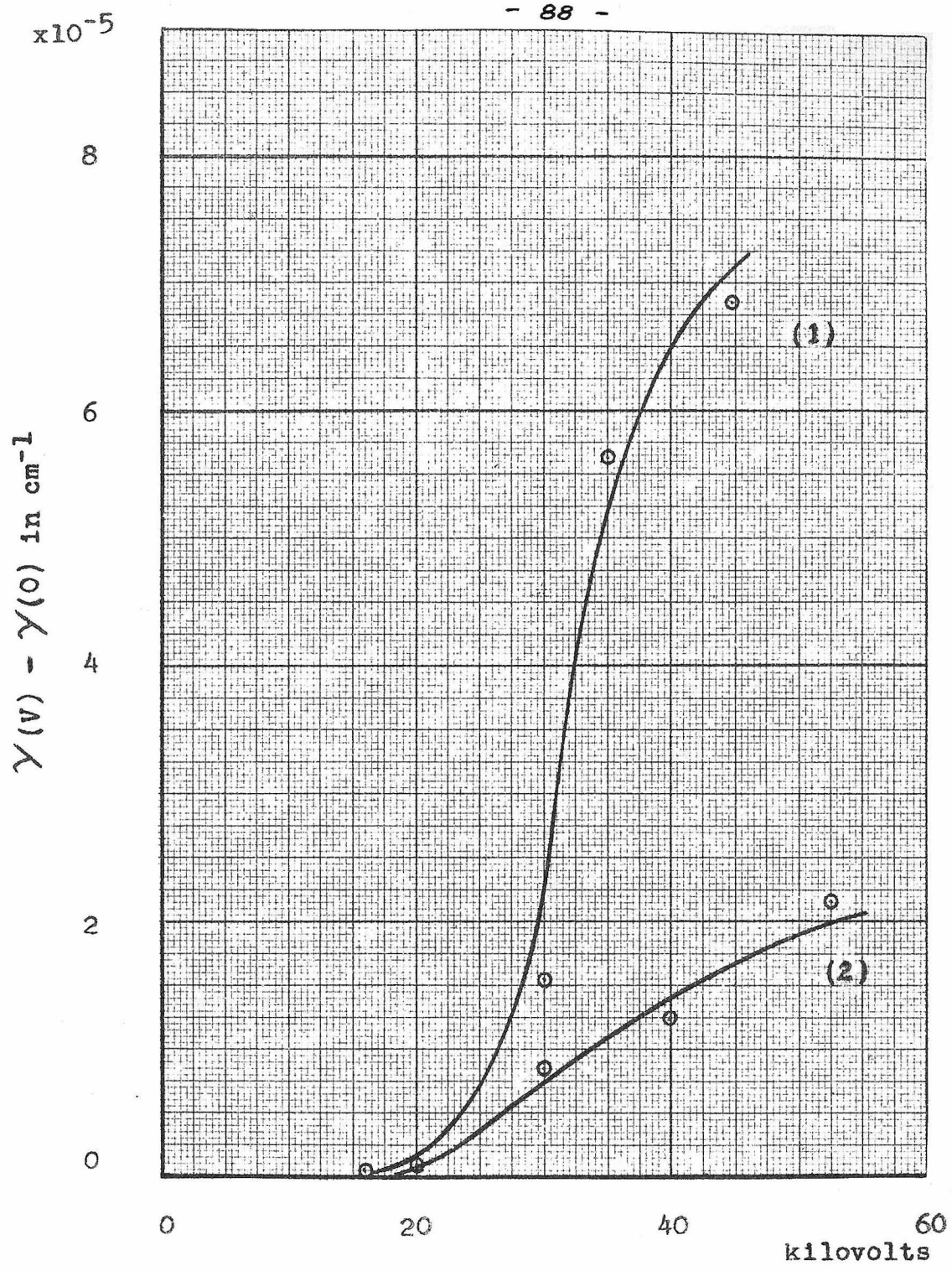

Figure 19. AMMONIA ABSORPTION VERSUS STARK VOLTAGE

100% NH_3 J=K=1 Res. at 42.8 kv
(1) p 102 cm Hg 8.766 kmc
(2) p 154 cm Hg 8.754 kmc

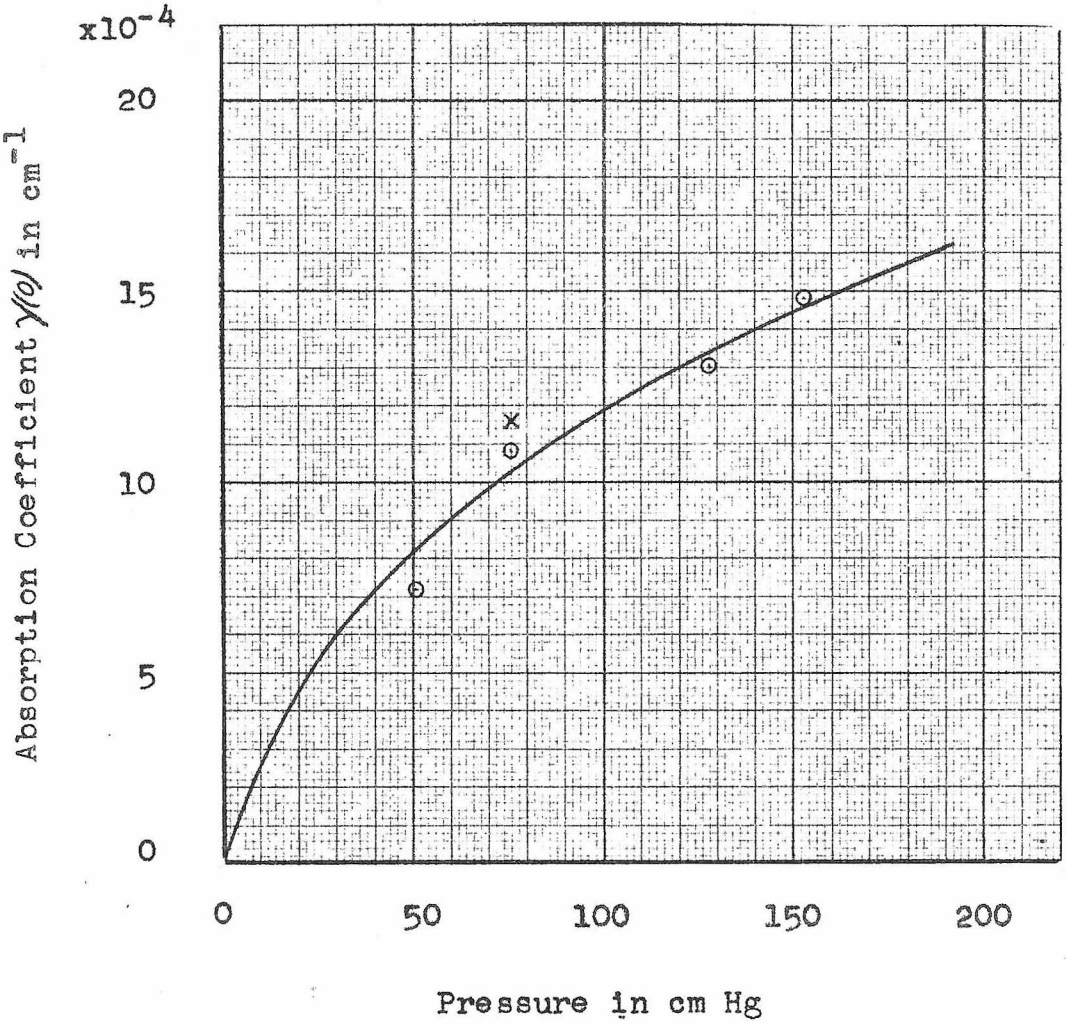

Figure 20. AMMONIA INVERSION ABSORPTION VERSUS PRESSURE

o This Thesis: $\nu_0 = 8.792$ to 8.754 kmc
x Cleeton & Williams: $\nu_0 = 8.8$ kmc

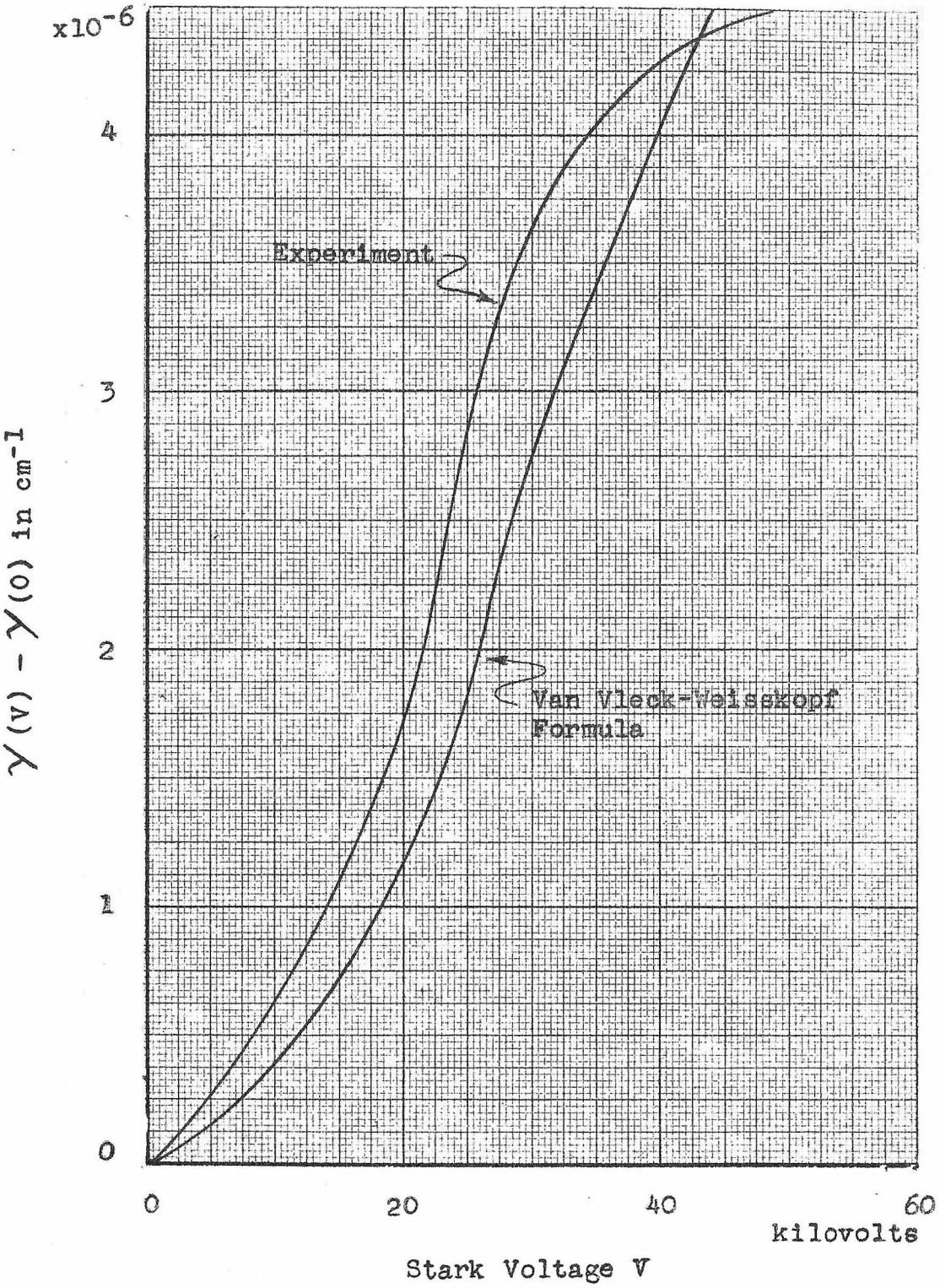

Figure 21. METHYL CHLORIDE ABSORPTION VERSUS STARK VOLTAGE

21.3 cm Hg
80% CH_3Cl
20% SF_6

$\nu_0 = 9.3535$ kmc
J=K=1 Res. at 33.1 kv

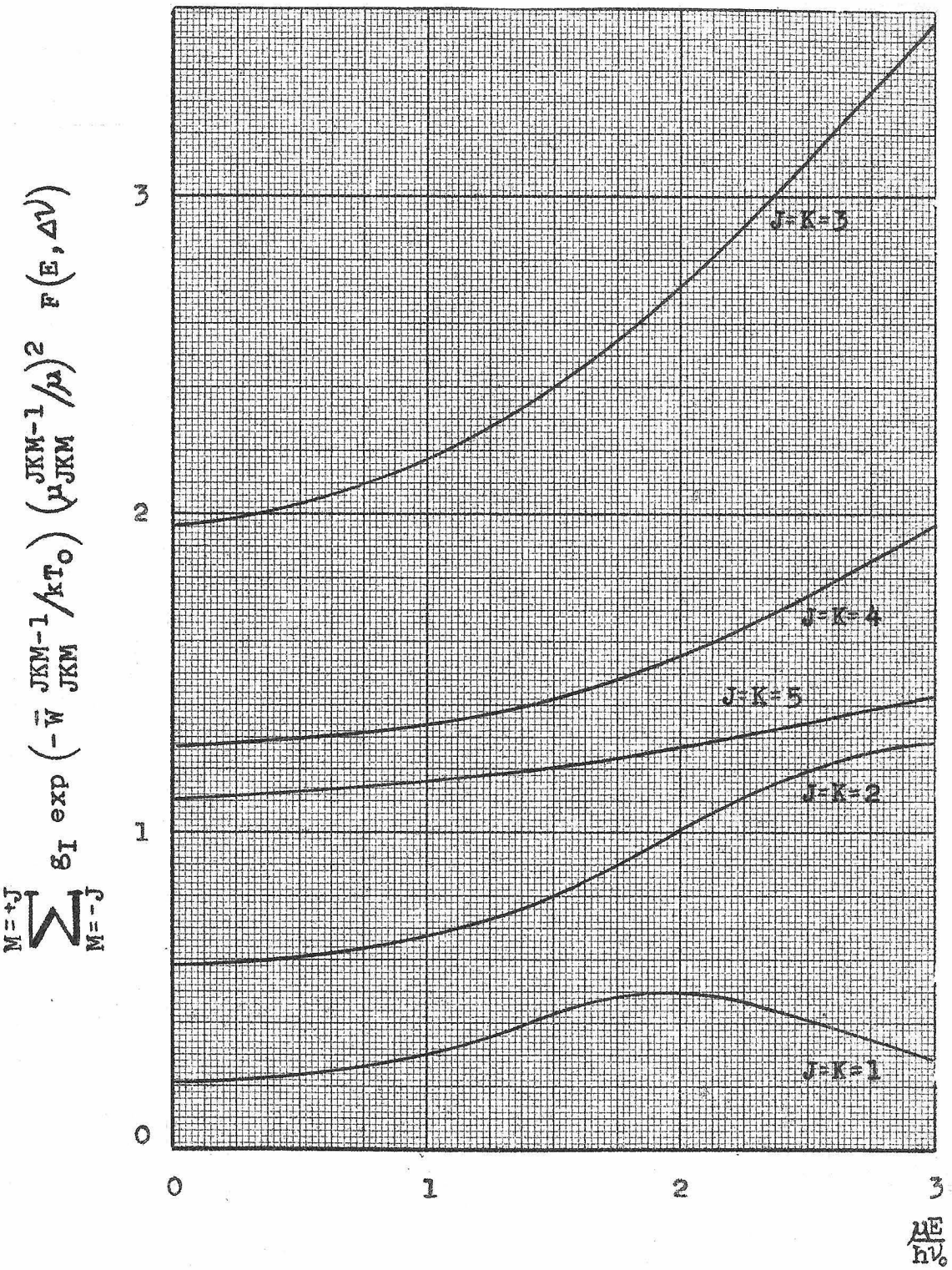

Figure 22. MEDIUM-BREADTH ABSORPTION LINES

J=K=1, 2, 3, 4, 5 $\quad \frac{\Delta\nu}{\nu_o} = 0.618$

	Frequency ν_o (kmc)	
Length d	Theory	Exp.
0.750 in	8.32	8.360
0.727	8.64	8.518
0.701	8.82	8.796
0.652	9.40	9.360

$a = 1.895$ in $\quad b_2 = 1.475$ in

$b_1 = 1.375$ in $\quad \delta = 0.0678$ in

Table 1. RESONANT CAVITY FREQUENCY

	NH_3	Ref.	CH_3Cl	Ref.
μ	1.45 Debyes	32	1.86 Debyes	32
A_o	189 kmc	33,p624	150 kmc	33,p618
B_o	298 kmc	33,p624	13.3 kmc	33,p618
σ_c	> 40 $\mathring{A}^2$?		1000 $\mathring{A}^2$?	2,p51
M	17.0 amu		50.5 amu	
I	1/2		1/2	
$\bar{\nu}_{lowest}$	$\bar{\nu}_2 = 932$ cm^{-1}	5,p295	$\bar{\nu}_3 = 732$ cm^{-1}	5,p315

Table 2. NH_3 and CH_3Cl PARAMETERS

IMPORTANT SYMBOLS AND ABBREVIATIONS

Latin Letter Symbols

A	Unique reciprocal moment of inertia for symmetric-top molecule, in sec^{-1}.
A_0	Average A for ground vibrational state.
a	Radius of resonant cavity.
B	Non-unique reciprocal moment of inertia for symmetric-top molecule, in sec^{-1}.
B_0	Average B for ground vibrational state.
c	Phase velocity of light, 2.998×10^{10} cm/sec.
d	Interelectrode spacing, or length of resonant cavity.
$\underset{\sim}{E}$	Static electric field vector.
E	Magnitude of E.
$F(E,\Delta\nu)$	Shape function given by $\dfrac{\frac{\Delta\nu}{\nu_0}}{\left[\frac{K}{J(J+1)}\frac{\mu E}{h\nu_0}-1\right]^2+\left[\frac{\Delta\nu}{\nu_0}\right]^2}+\dfrac{\frac{\Delta\nu}{\nu_0}}{\left[\frac{K}{J(J+1)}\frac{\mu E}{h\nu_0}+1\right]^2+\left[\frac{\Delta\nu}{\nu_0}\right]^2}$.
$f(\nu_i,\nu)$	Line-shape factor given by $\dfrac{\nu}{\pi\nu_i}\left[\dfrac{\Delta\nu}{(\nu_i-\nu)^2+(\Delta\nu)^2}+\dfrac{\Delta\nu}{(\nu_i+\nu)^2+(\Delta\nu)^2}\right]$.
Δf	Noise band width of parallel-T amplifier.
g_I	Statistical weight factor due to nuclear spin.
h	Planck's constant, 6.623×10^{-27} erg sec.
$\hbar$	$h/2\pi$.
I	Nuclear spin, in $\hbar$ units.

i	Index for totality of initial-state quantum numbers.
J	Total angular momentum quantum number.
ΔJ	J of final state minus J of initial state.
j	Index for totality of final-state quantum numbers.
K	Molecular spin quantum number, or projection of J on symmetry axis.
ΔK	K of final state minus K of initial state.
K	Resonant cavity coupling parameter given by $\mu^2 Z_0 / \pi_0 L$.
k	Boltzmann's constant, 1.380×10^{-16} ergs/deg.
M	Electric quantum number, or projection of J in static electric field direction.
ΔM	M of final state minus M of initial state.
M'	Modified crystal figure of merit given by $R_c / b \sqrt{2t R_c + R_a}$.
N	Number of molecules per unit volume.
P_a	Available microwave power into cavity.
Q	Resonant cavity unloaded (for K = 0, i.e., zero coupling to lines) quality factor with gas in absorption cell.
Q'	Loaded Q.
Q_o	Unloaded quality factor without gas.
Q_o'	Loaded Q_o.

ΔQ	Decrement in unloaded quality factor due to gas absorption, or $Q_o - Q$.
S	Cavity sensitivity factor defined by $\Delta\Gamma(\omega)/\gamma$.
T	Absolute temperature of test gas.
T_o	300°K.
V	Stark voltage, or voltage across cell electrodes.
v	Vibrational quantum number.
v_p	Phase velocity, not in free space.
$\bar{W}_i^j$	Average energy of i th and j th eigenstates.
$\Delta W_{JKM}^{(1)}$, $\Delta W_{JKM}^{(2)}$	Energy perturbation depending on E and E^2.

Greek Letter Symbols

α	Microwave attenuation factor from resonant cavity to detection crystal.
$\Delta\alpha$	Change in microwave calibrated attenuator for calibration purposes.
β	Phase constant in free space $\frac{\omega}{c}$, in cm^{-1}.
β'	Phase constant not in free space $\frac{\omega}{v_p}$, in cm^{-1}.
$\Gamma(\omega)$	Cavity transmission-loss function.
$\Delta\Gamma(\omega)$	Increment in $\Gamma(\omega)$ due to gas absorption.
γ	Linear absorption coefficient, in cm^{-1}.
γ_o	Maximum value of γ.
$\gamma(V)$	γ as a function of Stark voltage.
$\gamma(0)$	Zero-field value of γ, i.e., for $V = 0$

K	Dielectric constant of absorption-cell septum.
μ	Electric dipole moment of molecule in esu.
μ_{ij}	Electric dipole matrix element.
ν_0	Characteristic frequency of resonant cavity, or operating frequency ν of incident radiation.
ν_{ij}	Resonant frequency of a spectral line for transition between i th and j th eigen-states.
$\Delta\nu$	Line-breadth parameter, or half-breadth of spectral line at half-maximum.
$\bar{\nu}_s$	Fundamental vibrational frequency of a molecule for s-mode, in cm^{-1}.
p	Absorption-cell space factor, or ratio of microwave energy in cell to that in the entire cavity.
σ_c	Effective molecular collision cross section, in Å^2.

Abbreviations

F	Unit of frequency, 1 Fresnel $\equiv 10^{12}$ cycles per sec.
kmc	Unit of frequency, 1 kilomegacycle $\equiv 10^9$ cycles per sec.
Debye	Unit of electric moment, 1 Debye $\equiv 10^{-18}$ esu.
Å^2	Unit of area, 1 $\text{Å}^2 \equiv 10^{-16}$ cm^2.

REFERENCES

1. Cleeton, C. E. and Williams, N. H. Phys. Rev. (1934) 45 234.
2. Coles, D. K. "Scientific Paper No. 1407" (Westinghouse Research Laboratory, 1950).
3. Gordy, W. Rev. Mod. Phys. (1948) 20 668.
4. Debye, P. Polar Molecules (Dover Publications, 1945).
5. Herzberg, G. Infrared and Raman Spectra of Polyatomic Molecules (D. Van Nostrand, 1945).
6. Reiche, F. . Z. Physik (1926) 39 444.
7. de Kronig, R. and Rabi, I. I. Phys. Rev. (1927) 29 262.
8. Slawsky, Z. I. and Dennison, D. M. J. Chem. Phys. (1939) I 509.
9. Casimer, H. B. G. On the Interaction between Atomic Nuclei and Electrons (De Erven F. Bohn, Haarlem, 1936).
10. Van Vleck, J. H. Phys. Rev. (1947) 71 468A.
11. Van Vleck, J. H. Theory of Electric and Magnetic Susceptibilities (Clarendon Press, Oxford, 1932) Ch. VI.
12. de Kronig, R. Proc. Nat. Acad. Sci. (1926) 12 608.
13. Hughes, H. K. Phys. Rev. (1947) 72 614.
14. Heitler, W. The Quantum Theory of Radiation (Oxford Univ. Press, 1944).
15. Weisskopf, V. F. Physikalische Zeitschrift (1933) 34 1.
16. Karplus, R. Phys. Rev. (1948) 73 1120.
17. Van Vleck, J. H. and Weisskopf, V. F. Rev. Mod. Phys. (1945) 17 227.
18. Reiche, F. and Rademacker, H. Z. Physik (1927) 41 453.
19. Dennison, D. M. Phys. Rev. (1926) 28 318.
20. Dennison, D. M. Rev. Mod. Phys. (1931) 3 280.

REFERENCES, Continued.

21. Van Vleck, J. H. Phys. Rev. (1947) 71 413.

22 Bleaney, B. and Penrose, R. P. Nature (1946) 157 339.

23 Cobine, J. D. Gaseous Conductors (McGraw Hill 1941) 163.

24. Smythe, W. R. Static and Dynamic Electricity (2nd Ed. McGraw Hill, 1950).

25. Maxstadt, F. W. Elec. Eng. (1934) 53 1063.

26. Dicke, R. H. Rev. Sci. Inst. (1946) 17 268.

27. Dicke, R. H. et al. Phys. Rev. (1946) 70 340.

28. Stutt, C. A. "Tech. Report No. 105" (Rad. Lab. of Electronics, M. I. T., March, 1949).

29. Montgomery, C. G. et al. Principles of Microwave Circuits (McGraw Hill 1948) Ch. 7.

30. Torrey, W. C. and Whitmer, C. A. Crystal Rectifiers (McGraw Hill 1948).

31. "Progress Report, July 1, 1948" (Lab. of Nuclear Science and Eng.) p. 36.

32. Wesson, L. G. Tables of Electric Dipole Moments (Technology Press, M. I. T., 1948).

33. Kisliuk, P. and Townes, C. H. National Bureau of Standards Journal of Research (1950) 44 611.

34. Dennison, D. M. and Uhlenbeck, G. E. Phys. Rev. (1932) 41 313.

35. Anderson, P. W. Phys. Rev. (1949) 76 647.

36. Zaviosky, E. J. Phys. U.S.S.R. (1945) 9 211, 245, 447; (1946) 10 170, 197.

37. Cummerow, R. L. and Halliday, D. Phys. Rev. (1946) 70 433.

38. Surber, W. H. J. App. Phys. (1948) 19 514.